

RESEARCH MEMORANDUM

PRELIMINARY INVESTIGATION OF VARIOUS AILERONS ON
A 42° SWEPTBACK WING FOR LATERAL CONTROL AT
TRANSONIC SPEEDS

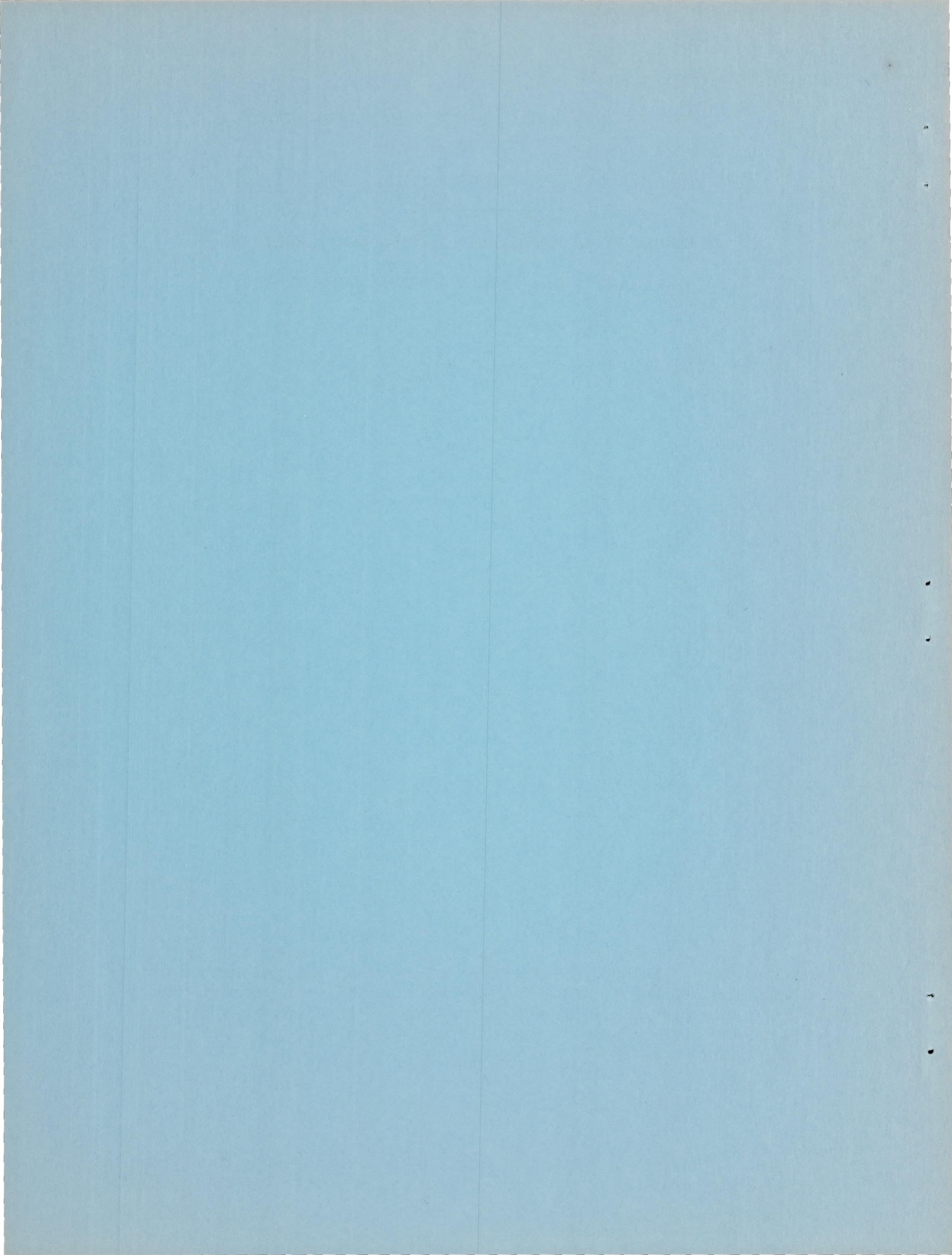
By

Thomas R. Turner, Vernard E. Lockwood,
and Raymond D. Vogler

Langley Aeronautical Laboratory
Langley Field, Va.

NATIONAL ADVISORY COMMITTEE
FOR AERONAUTICS
WASHINGTON

September 7, 1948
Declassified August 18, 1954



NATIONAL ADVISORY COMMITTEE FOR AERONAUTICS

RESEARCH MEMORANDUM

PRELIMINARY INVESTIGATION OF VARIOUS AILERONS ON
A 42° SWEEPBACK WING FOR LATERAL CONTROL AT
TRANSONIC SPEEDS

By Thomas R. Turner, Vernard E. Lockwood,
and Raymond D. Vogler

SUMMARY

An investigation at transonic speeds has been performed in the Langley high-speed 7- by 10-foot tunnel to determine the rolling-effectiveness characteristics of several aileron arrangements for use on a 42° sweptback wing. The tests were performed on a small model of a 42° sweptback wing by a method similar to the NACA wing-flow method. The testing technique involved placing a small model in the high-velocity flow field generated over a curved surface. The investigation was concerned primarily with modifications to the regular aileron chord and contour to obtain an aileron which would not show reversal of effectiveness in the transonic speed range. In addition, some unconventional-type ailerons, such as spoilers and auxiliary lifting surfaces, were tested. No attempt has been made to analyze the data fully.

The data presented indicated the effectiveness of the original 0.20-chord circular-arc aileron reversed from a Mach number of 0.92 to 1.175 for a deflection of 2.3° . For higher deflections the effectiveness approached zero at higher Mach numbers. Neither the flat-sided nor the cusp normal-chord aileron showed much improvement in effectiveness at low deflections over the circular-arc aileron. Extending the chord of the aileron improved control throughout the speed range investigated.

The parallel-sided aileron (an unconventional aileron of uniform chord thickness) showed no indication of reversal and had better effectiveness than either of the other normal-chord ailerons tested. A spoiler deflection of 1 percent and 5 percent chord appeared to be quite an effective means of control up to a Mach number of 1.15 with no indication of reversal.

INTRODUCTION

One of the many problems arising from the use of sweptback wings on high-speed aircraft has been that of securing adequate lateral control,

particularly in the transonic speed range. It was the purpose of this investigation to aid in finding a suitable aileron which would offer positive control throughout the transonic speed range.

In order to obtain a solution to the problem of lateral control, a small 42° sweptback wing was built and tested on the transonic bump. The effect of aileron profile, chord, and span was determined. In addition, a limited number of tests were made to determine the effectiveness of spoilers, auxiliary airfoils, and leading-edge flaps in connection with aileron deflection as lateral control devices.

It was not the purpose of the present investigation to obtain complete data on the various configurations investigated but only to determine their acceptability as controls in the transonic speed range. The only data obtained were the rolling-moment coefficients; thus, the effects of the unconventional ailerons on the other aerodynamic characteristics have yet to be investigated.

SYMBOLS AND CORRECTIONS

C_{l_a}	rolling-moment coefficient produced by aileron (L'/qSb)
δ_a	aileron deflection, positive when trailing edge is down
\bar{c}	wing mean aerodynamic chord (M.A.C.), 0.25 foot
b	twice span of semispan model, 1 foot
S	twice area of semispan model, 0.25 square foot
L'	model rolling moment produced by aileron about plane of symmetry, foot-pounds
q	average dynamic pressure over span of model
ρ	mass density of air, slugs per cubic foot
M	average Mach number over span of model
M_T	tunnel reference Mach number
M_l	local Mach number
R	Reynolds number

Subscripts:

o outboard

i inboard

f.s. full span

The data have been corrected in accordance with reference 1 for reflection-plane models. This correction is for extremely low Mach numbers. No correction has been made for Mach number effect. The corrections applied were as follows:

$$C_{l_a} = C_{l_{\text{measured}}} \times 0.897, \text{ for outboard ailerons}$$

$$C_{l_a} = C_{l_{\text{measured}}} \times 0.765, \text{ for full-span ailerons}$$

$$C_{l_a} = C_{l_{\text{measured}}} \times 0.759, \text{ for inboard ailerons}$$

No correction was applied to the data for the wing-tip aileron.

TESTING TECHNIQUE

The tests were performed in the Langley high-speed 7- by 10-foot tunnel which is a closed-throat, single-return tunnel capable of reaching the choking Mach number. In order to obtain transonic speeds in the tunnel, an application of the NACA wing-flow method of testing (reference 2) was made. This method of testing at transonic speeds involves placing the model in the high-velocity flow field generated over the curved surface of a bump on the tunnel floor (fig. 1). A sketch showing the relative location of the model on the bump is given in figure 2. An electrical strain gage is mounted in a chamber in the bump and measures only the rolling moment of the model about the plane of symmetry of the model. This chamber is sealed except for a hole through which the butt of the wing passes. The fuselage which was approximately 1/32 inch above the bump surface covered this hole.

All of the tests were run at approximately 0° angle of attack.

Figure 3 shows the variation of the local Mach number along the surface (chordwise) of the bump in the vicinity of the model and the vertical variation for a position near the leading edge of the wing root. The test Mach number was the average Mach number over the span of the model. The average Mach number over the span of the model is higher than the average Mach number over the span of the aileron by approximately 0.01 at the lowest Mach number and 0.03 at the highest Mach number tested (fig. 3). No attempt has been made to evaluate the effect of the variation in Mach number along the chord and span of the

model. The variation of Reynolds number with Mach number for test conditions is presented in figure 4.

MODEL

The semispan model used for these tests had 42.8° of sweepback, taper ratio of 0.50, and aspect ratio of 4.0; other geometric characteristics are shown in figure 5. The wing was a 10-percent-thick circular-arc section normal to the 50-percent-chord line, had no dihedral, and was mounted as a midwing (fig. 5). The fuselage was semicircular in cross section. The wing was of polished steel and the fuselage of polished brass.

The ailerons were attached to the wing with a $\frac{1}{32}$ -inch-thick copper insert (fig. 5). This insert was bent to obtain the required deflection. The deflection was checked before and after each test. For the sealed condition the gap between wing and aileron was filled with beeswax and faired. For the unsealed tests the beeswax was left out, the leading edges of aileron were slightly rounded, and the copper insert was replaced with a steel insert with $\frac{1}{32}$ -inch holes drilled $\frac{1}{16}$ inch on centers spanwise between aileron and wing.

Some of the more important geometric characteristics of the models tested including the trailing-edge angles as measured parallel to the plane of symmetry are given in the following table (the aileron chord is based on the original wing chord in all cases):

Aileron chord, percent wing chord	Description	Approximate trailing-edge angle parallel to plane of symmetry
20	Circular arc	20.0
20	Flat sides	16.0
20	Cusp	7.2
26.9	Flat sides	11.7
26.9	Cusp	9.0
32	Flat sides	10.0
40	Flat sides	7.0
20	Parallel sides	-----

In addition, wing-tip and triangular inboard ailerons were tested. The geometry of these unconventional ailerons is shown in figure 6.

RESULTS AND DISCUSSION

The rolling-moment coefficients presented in this paper are incremental, the coefficient at a given deflection minus the coefficient at zero deflection.

The variation of rolling-moment coefficient with Mach number for the normal-chord (0.20c) circular-arc aileron is presented in figures 7 to 9. Both the full-span and inboard ailerons (figs. 7 and 8) showed reversal of effectiveness for all deflections tested between Mach numbers of 0.925 and 1.175, the highest value tested. The outboard aileron (fig. 9) indicated reversal for a 2.3° deflection at a Mach number of 0.92. The aileron effectiveness for higher deflections approached zero at highest Mach numbers.

The variation of the rolling-moment coefficient with Mach number for the flat-sided aileron is presented in figures 10 to 12. The full-span aileron showed reversal for all deflections tested. The outboard aileron indicated zero effectiveness for deflections of 1.7° and 4.8° at a Mach number of 1.03 with some tendency to recover as the Mach number increased. At higher deflections, the flat-sided aileron appeared to be more effective than the circular-arc aileron. The inboard-aileron section had a negligible effect on the characteristics of the outboard aileron (figs. 11 and 12).

The outboard cusp aileron (fig. 13) appeared to be quite ineffective throughout the Mach number range tested for a 1.9° deflection, with reversal indicated at a Mach number of 0.905. The other deflections showed reasonable effectiveness throughout the Mach number range tested.

The results for the 0.269-chord cusp and flat-sided ailerons are presented in figures 14 and 15. It appears that the cusp aileron has the better characteristics. The variation of rolling-moment coefficient with Mach number for the 0.269-chord cusp aileron is similar to that of the 0.20-chord cusp aileron of figure 13, but because of the longer chord the aileron was more effective.

The results for the 0.32- and 0.40-chord flat-sided ailerons (figs. 16 and 17) show very similar characteristics and indicate no reversal up to $M = 1.175$, the highest tested. Both ailerons appeared to have better characteristics than the two smaller flat-sided ailerons tested.

Conditions along the hinge line appeared to affect the effectiveness of the ailerons tested. Removing the fairing at the hinge line (fig. 18) but maintaining the seal increased the aileron effectiveness up to a Mach number of 1.0; above this Mach number the effect was negligible. Leakage along the hinge line for either the 0.20-chord circular-arc or

the 0.40-chord flat-sided aileron (figs. 19 and 20) reduced the aileron effectiveness at most speeds and also reduced the variation of rolling-moment coefficient with Mach number. These results indicated that further studies of leakage along the hinge should be made in the transonic speed range.

Because it was thought that the reversal or ineffectiveness of the flat-sided or cusp 0.20-chord aileron might be a result of flow separation ahead of or near the hinge line of the aileron, an aileron was built that had constant thickness behind the hinge line. This contour would tend to fill up this area of separation or the reduced pressure gradient over the trailing edge might prevent separation when the aileron is neutral, and the control therefore should be effective for small deflections. The results for this aileron (fig. 21) showed no tendency for the effectiveness to reverse even for small deflections up to Mach numbers of 1.125, the highest tested. Furthermore, the effectiveness of this aileron was greater than that of the circular-arc, the flat-sided, or the cusp 0.20-chord ailerons.

Spoilers have shown good effectiveness on a very thin wing of about the same sweep and plan form at transonic speeds (reference 3). A spoiler arrangement that showed characteristics at low speed similar to the spoiler arrangement of reference 3 was tested at both 1- and 5-percent projection (fig. 22) and, as did the spoiler of reference 3, showed quite high effectiveness at all Mach numbers investigated.

Since leading-edge flaps deflected opposite to the ailerons have shown good effectiveness at Mach numbers above 1.5, they were investigated at the transonic speeds. At Mach numbers up to 1.15, the 0.15-chord leading-edge flap deflected either -5° or -10° (figs. 23 and 24) had a detrimental effect on the aileron characteristics.

One isolated test of a wing-tip aileron is presented in figure 25. For this arrangement, the aileron effectiveness was relatively good; however, this aileron will require considerable additional work.

The variation of rolling-moment coefficient with Mach number for a triangular inboard aileron designed to affect a large portion of the wing at supersonic speeds is presented in figure 26. This configuration showed reasonable effectiveness throughout the speed range tested; however, optimum shape and location have yet to be determined.

CONCLUSIONS

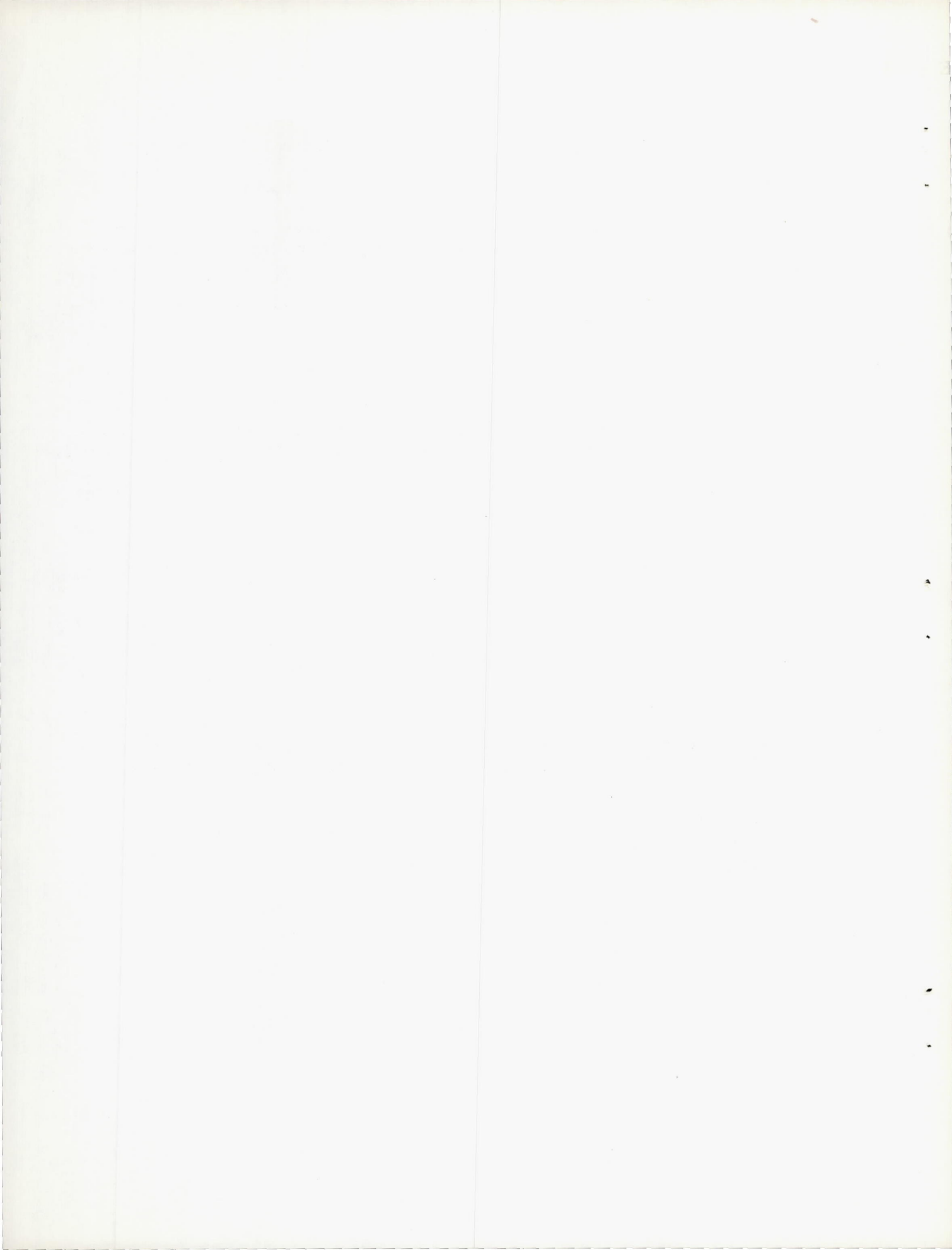
The results of tests at transonic speeds of a semispan 42° sweptback wing-fuselage combination indicate the following conclusions:

1. The normal aileron (0.20c circular arc) indicated reversal for a deflection of 2.3° at a Mach number of 0.92. For higher deflections, the effectiveness approached zero at higher Mach numbers.
2. Neither the flat-sided nor the cusp normal-chord aileron showed much improvement in effectiveness at low deflections over the circular-arc aileron.
3. Extending the chord of the aileron offered one method of providing positive control up to the highest Mach numbers tested.
4. Leakage along the hinge line had an important effect on the characteristics and should be investigated further.
5. The parallel-sided aileron showed no indication of reversal and greater effectiveness than either of the other normal-chord ailerons tested.
6. The spoilers were quite effective throughout the Mach number range tested.

Langley Aeronautical Laboratory
National Advisory Committee for Aeronautics
Langley Field, Va.

REFERENCES

1. Swanson, Robert S., and Toll, Thomas A.: Jet-Boundary Corrections for Reflection-Plane Models in Rectangular Wind Tunnels. NACA Rep. No. 770, 1943.
2. Gilruth, R. R., and Wetmore, J. W.: Preliminary Tests of Several Airfoil Models in the Transonic Speed Range. NACA ACR No. L5E08, 1945.
3. Schneider, Leslie E., and Ziff, Howard L.: Preliminary Investigation of Spoiler Lateral Control on a 42° Sweptback Wing at Transonic Speeds. NACA RM No. L7F19, 1947.



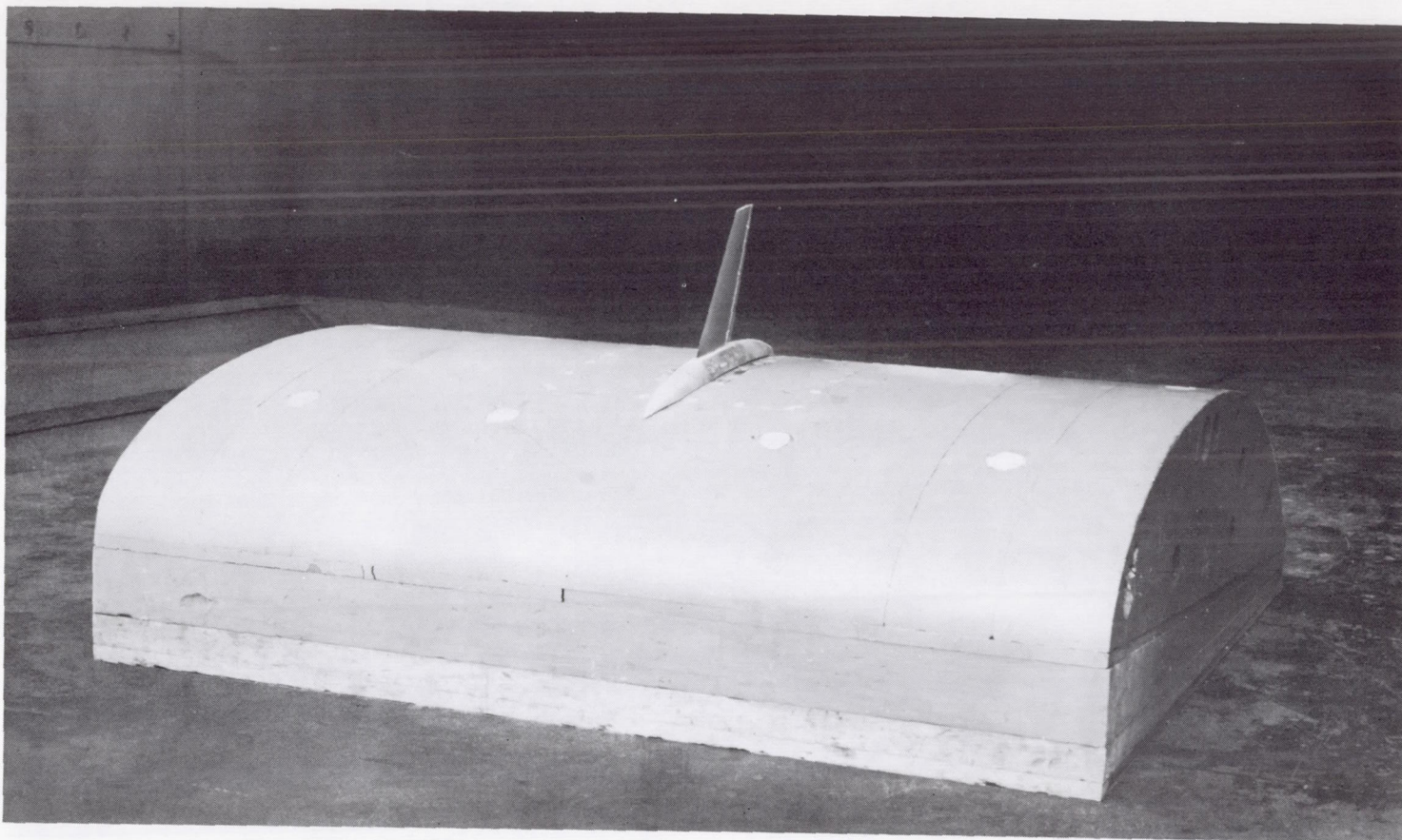
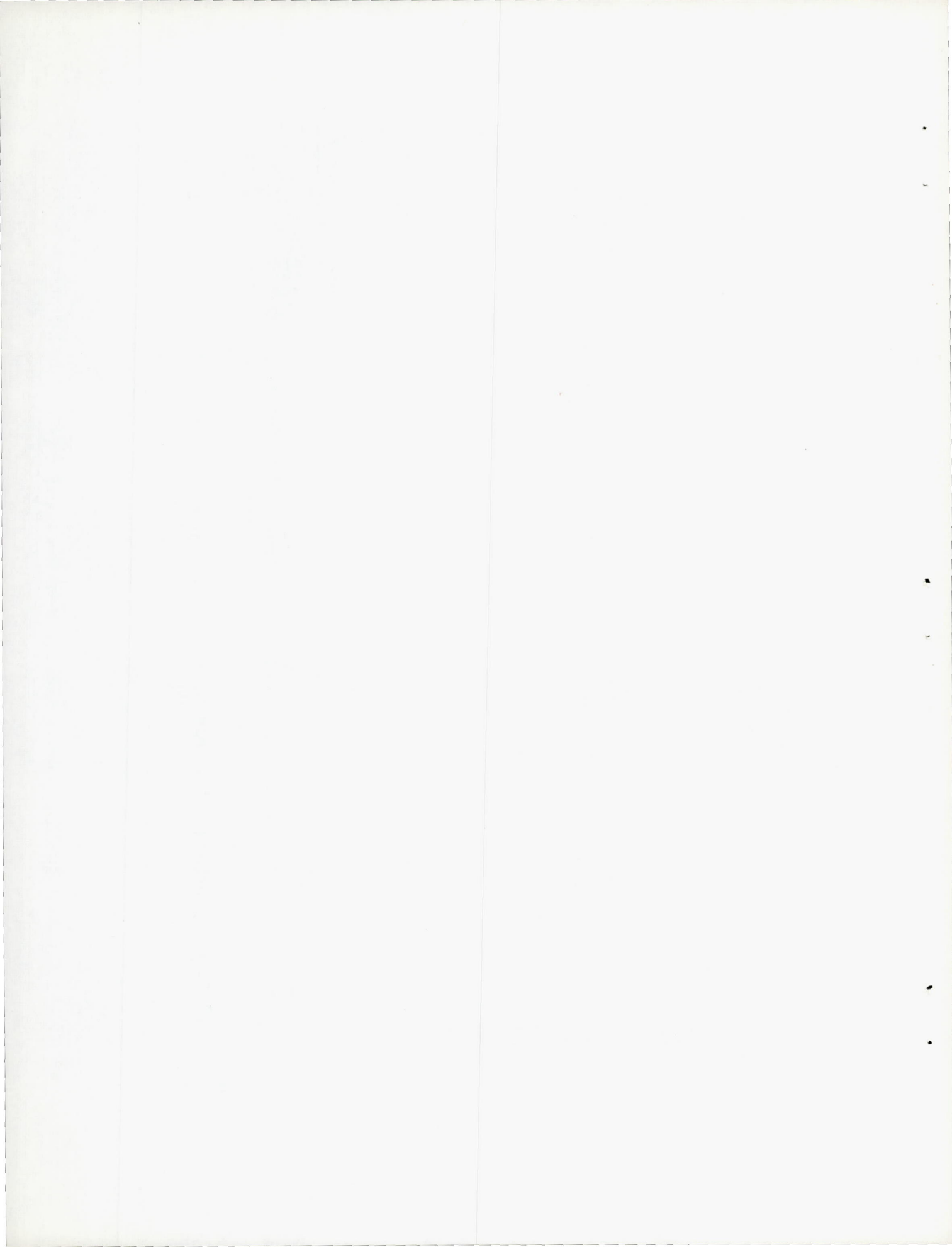


Figure 1.- Three-quarter front view of the model as mounted on the bump in the Langley high-speed 7- by 10-foot tunnel.



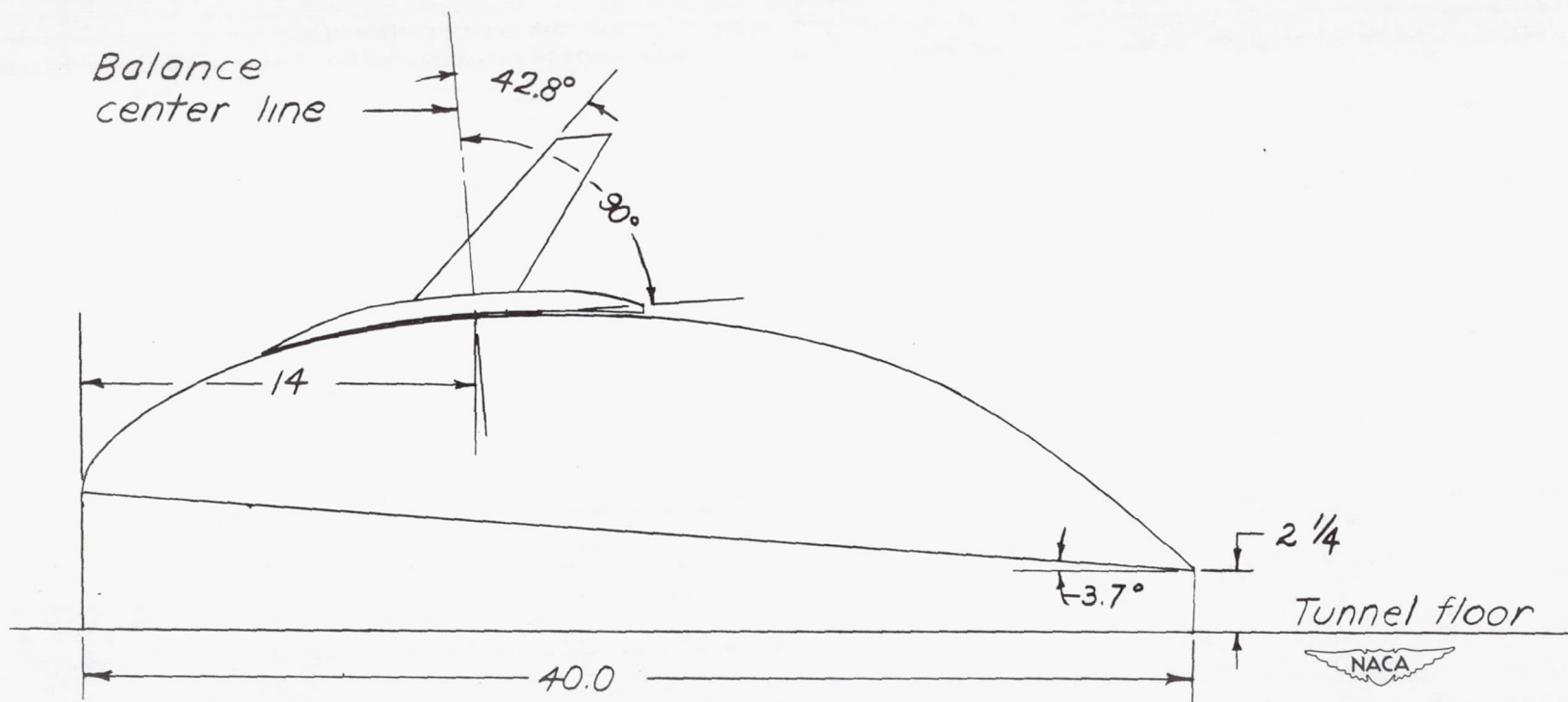


Figure 2.- Schematic sketch of relative position of model, balance, and transonic bump as mounted in the Langley high-speed 7- by 10-foot tunnel.

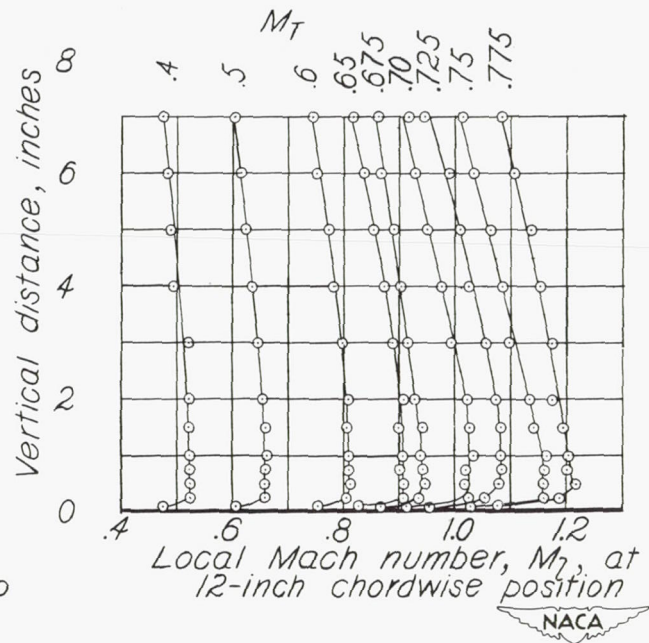
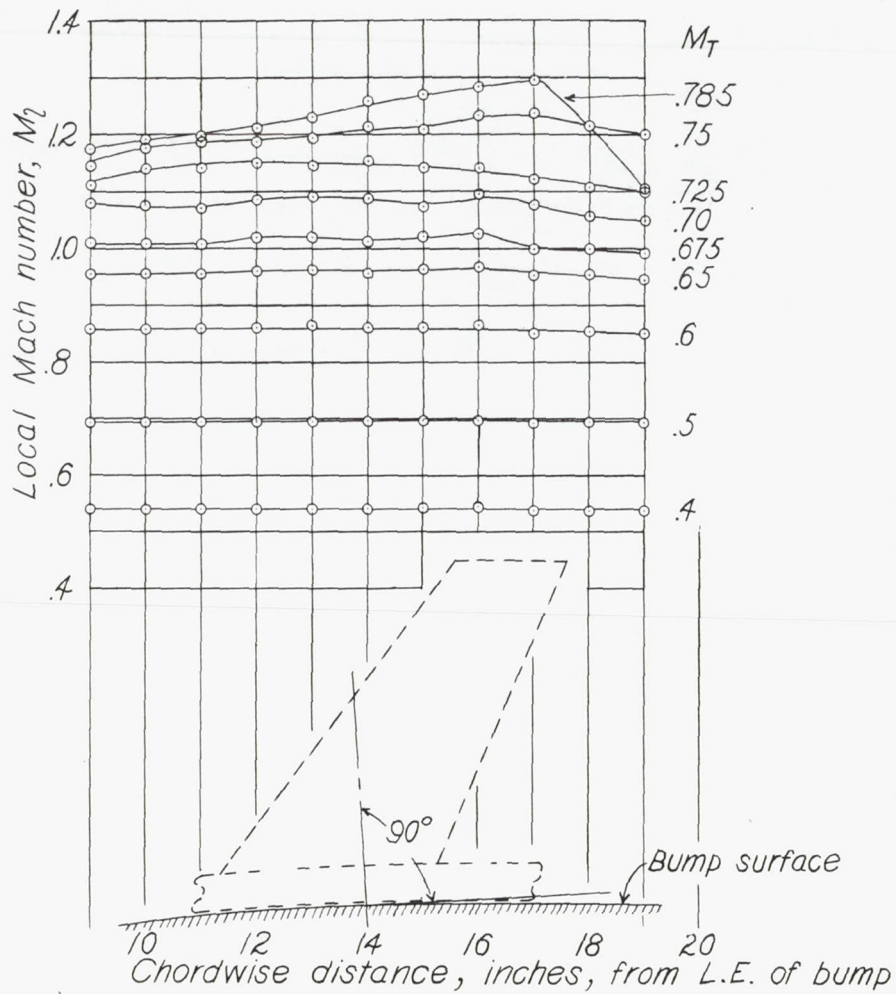


Figure 3.- Spanwise and chordwise distribution of Mach number over transonic bump. Model off.

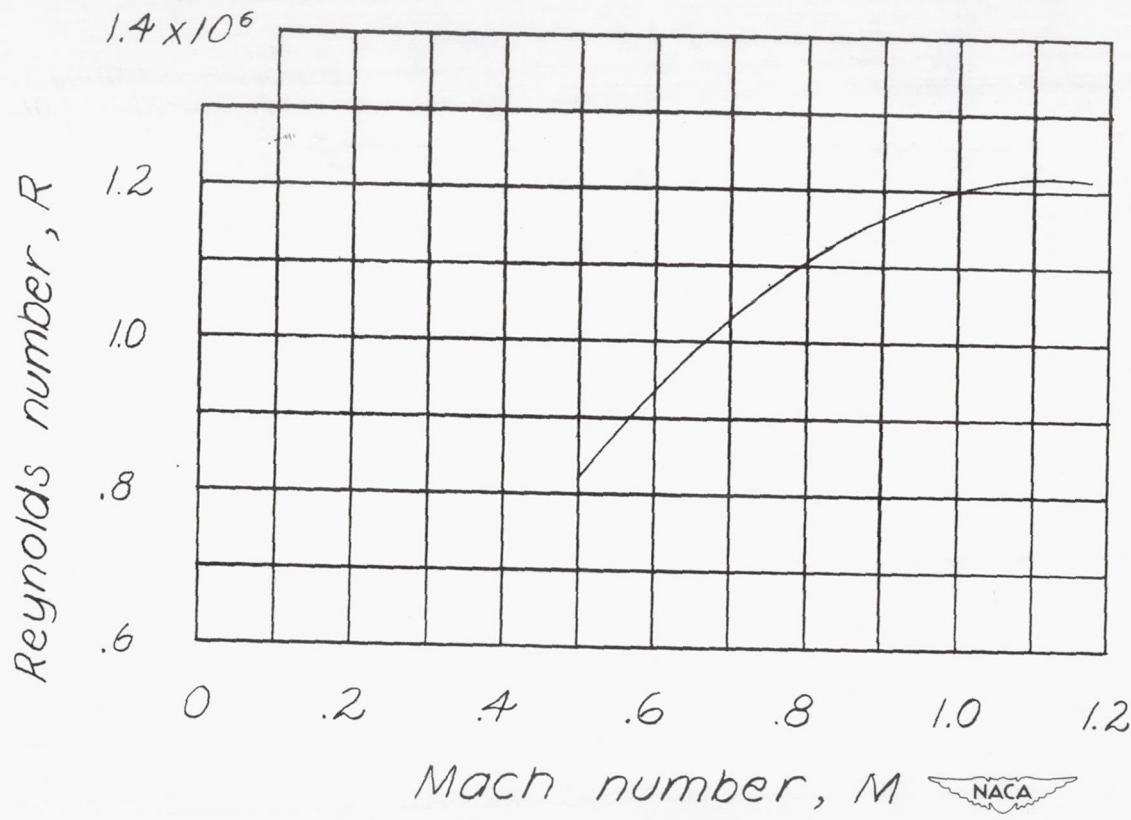


Figure 4.- Variation of Reynolds number with test Mach number. Reynolds number based on model mean aerodynamic chord of 0.25 foot.

Typical section

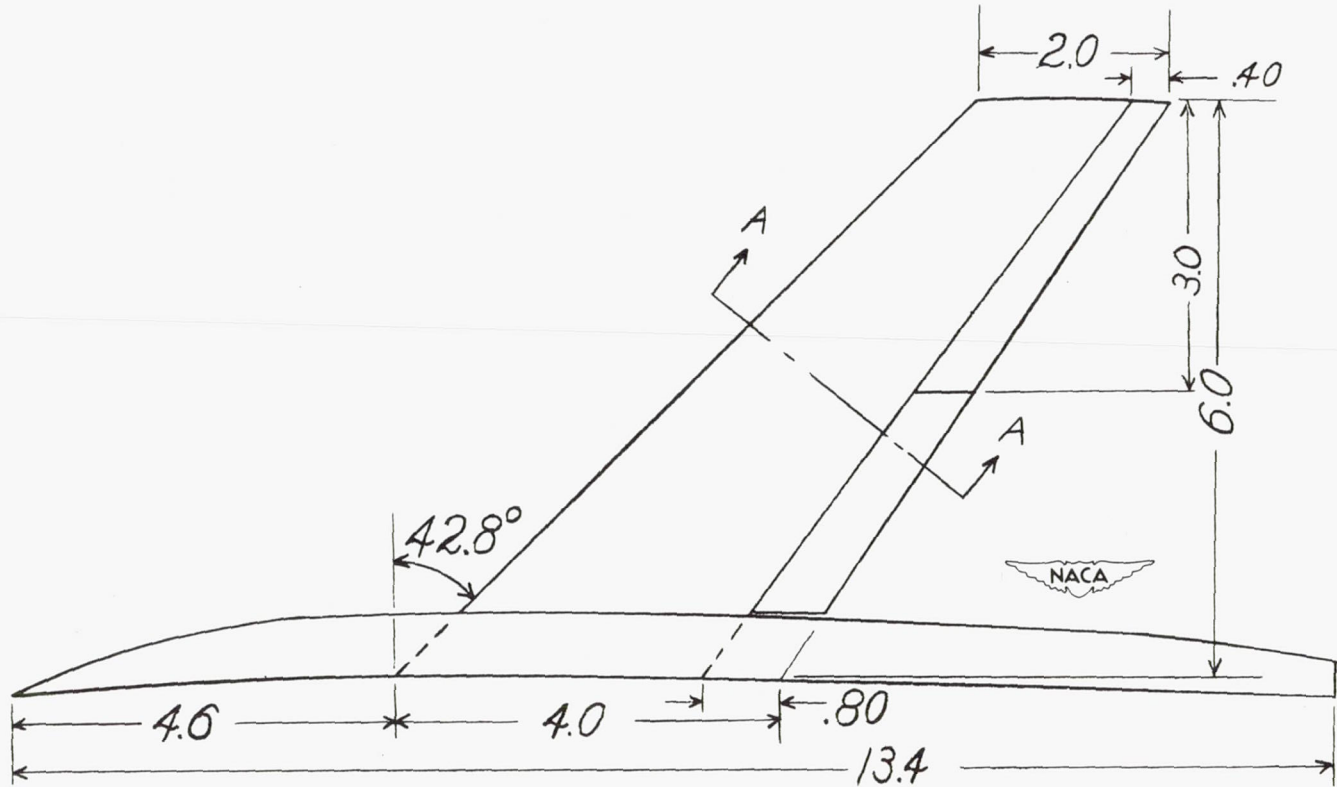
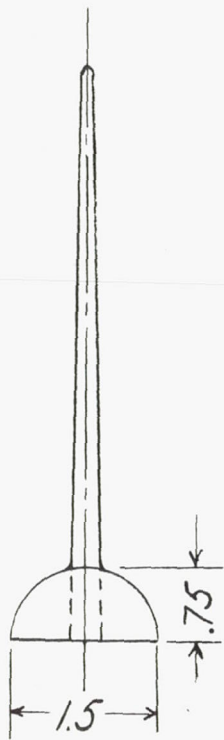
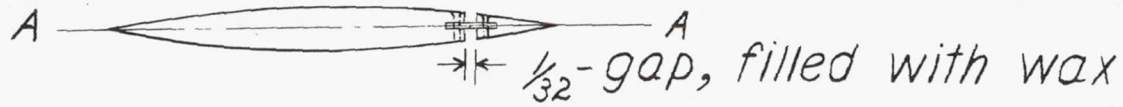
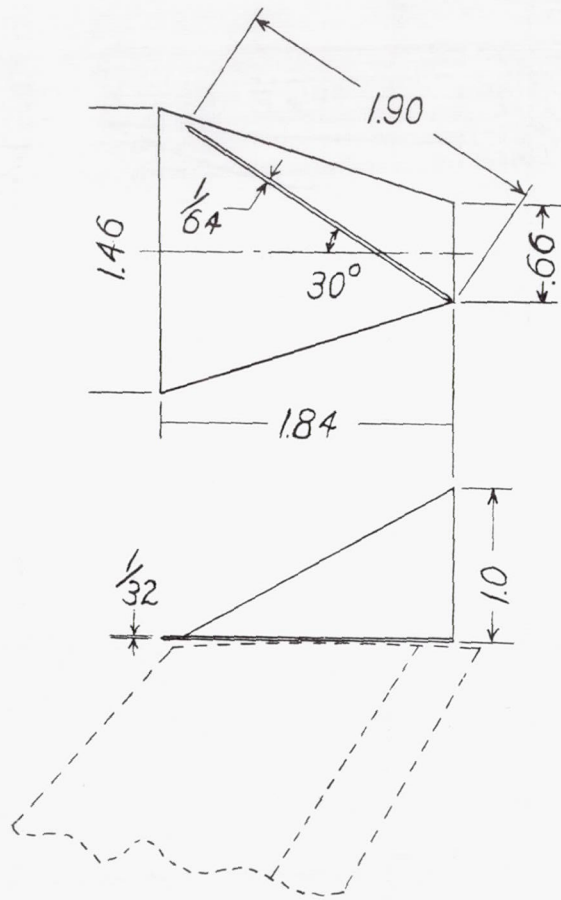
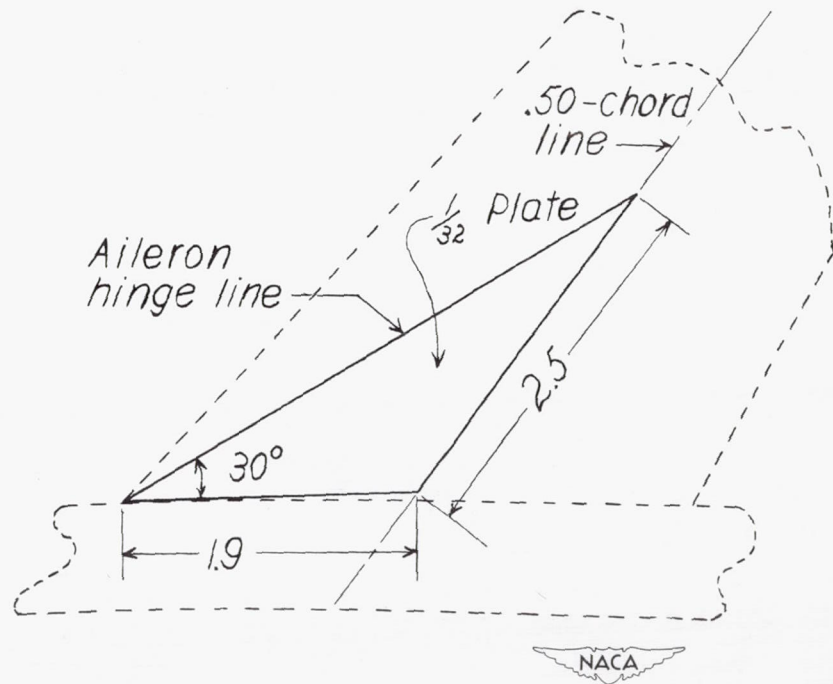


Figure 5.- Drawing of the 42.8° sweptback wing and fuselage combination.



(a) Wing-tip triangular aileron.



(b) Triangular inboard aileron.

Figure 6.- Drawings of wing-tip aileron and triangular inboard aileron.

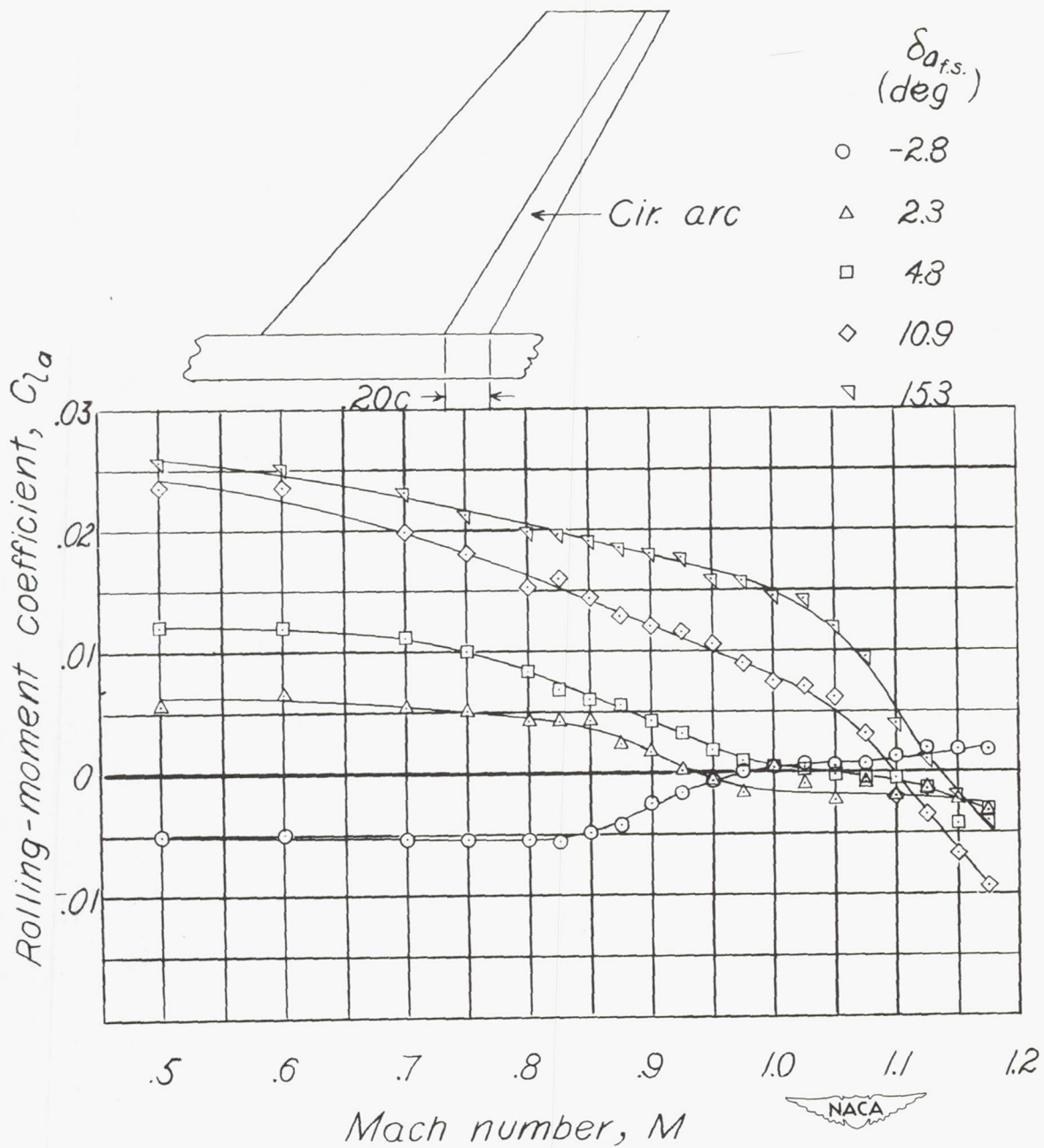


Figure 7.- Variation of rolling-moment coefficient with Mach number for a 0.20-chord full-span circular-arc aileron.

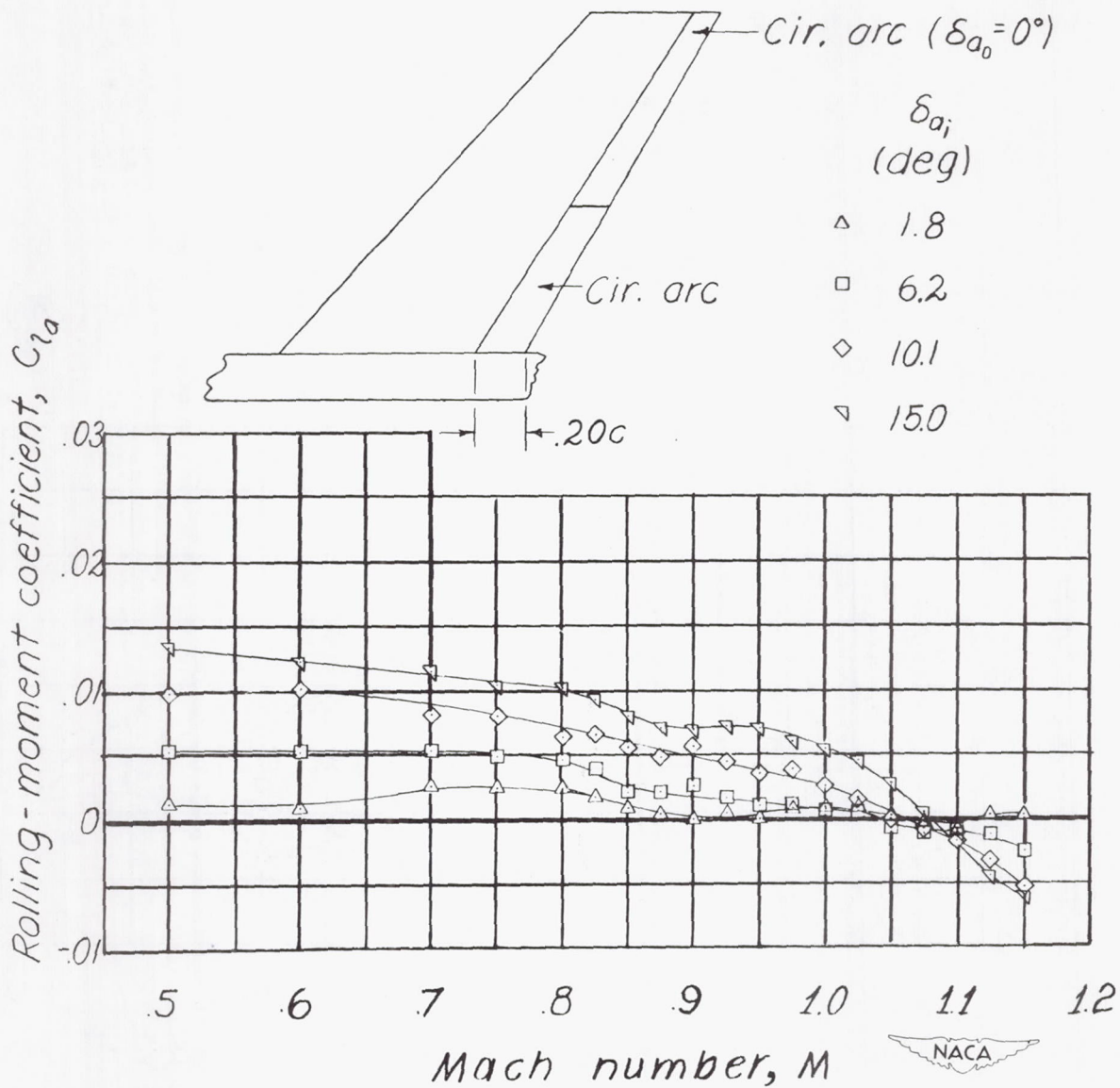


Figure 8.- Variation of rolling-moment coefficient with Mach number for a 0.20-chord circular-arc inboard aileron.

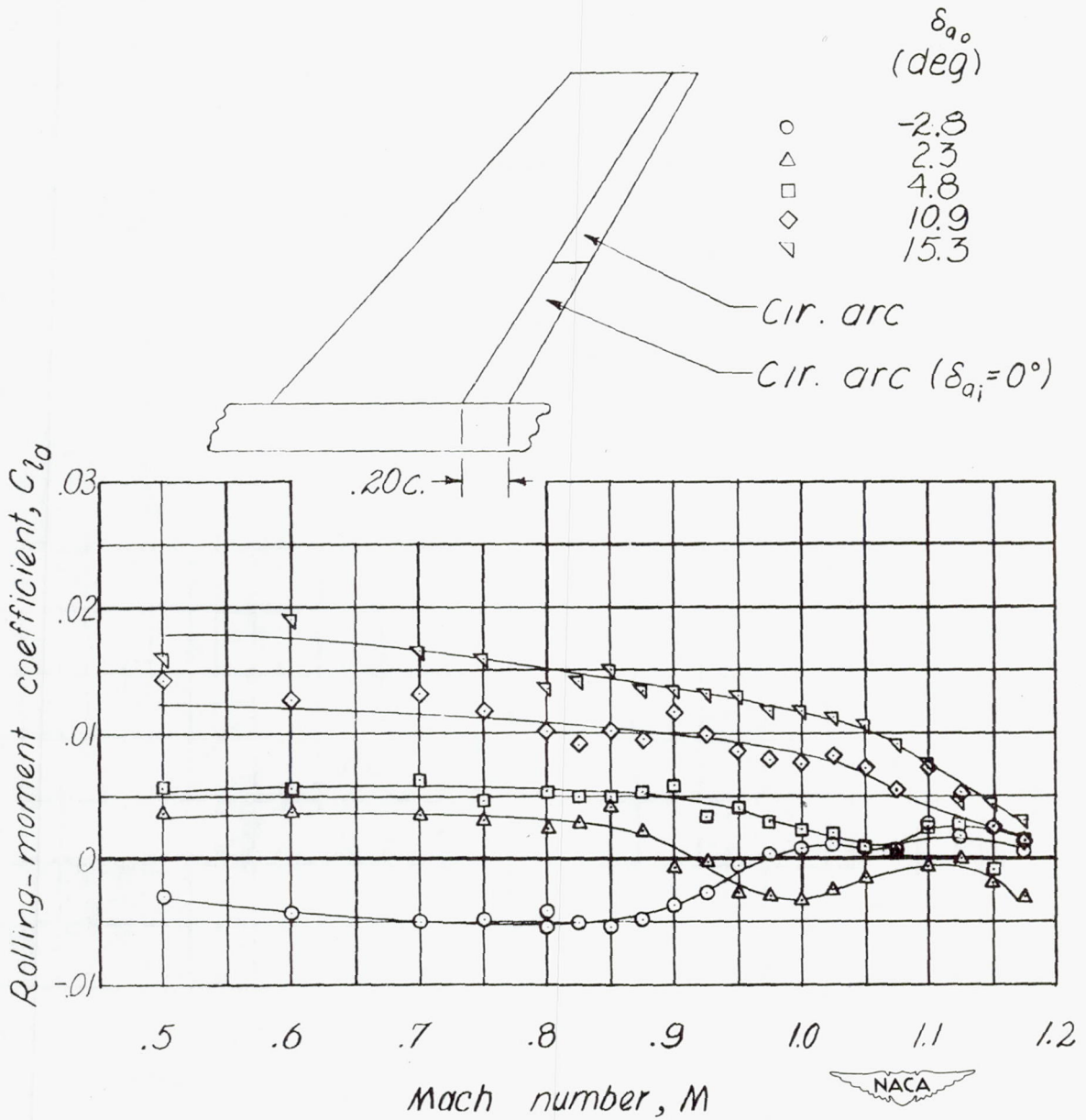


Figure 9.- Variation of rolling-moment coefficient with Mach number for a 0.20-chord circular-arc outboard aileron.

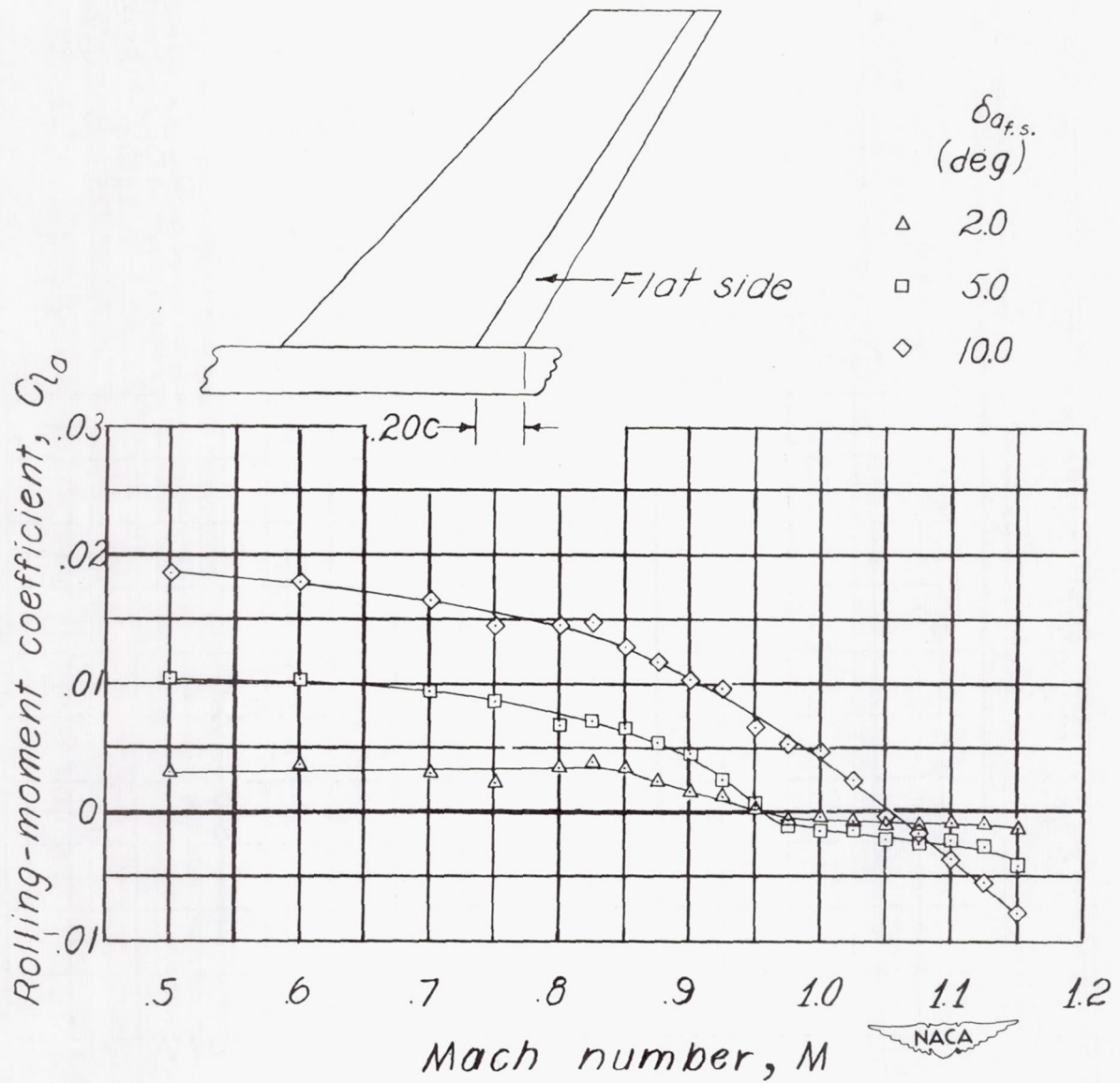


Figure 10.- Variation of rolling-moment coefficient with Mach number for a 0.20-chord flat-sided full-span aileron.

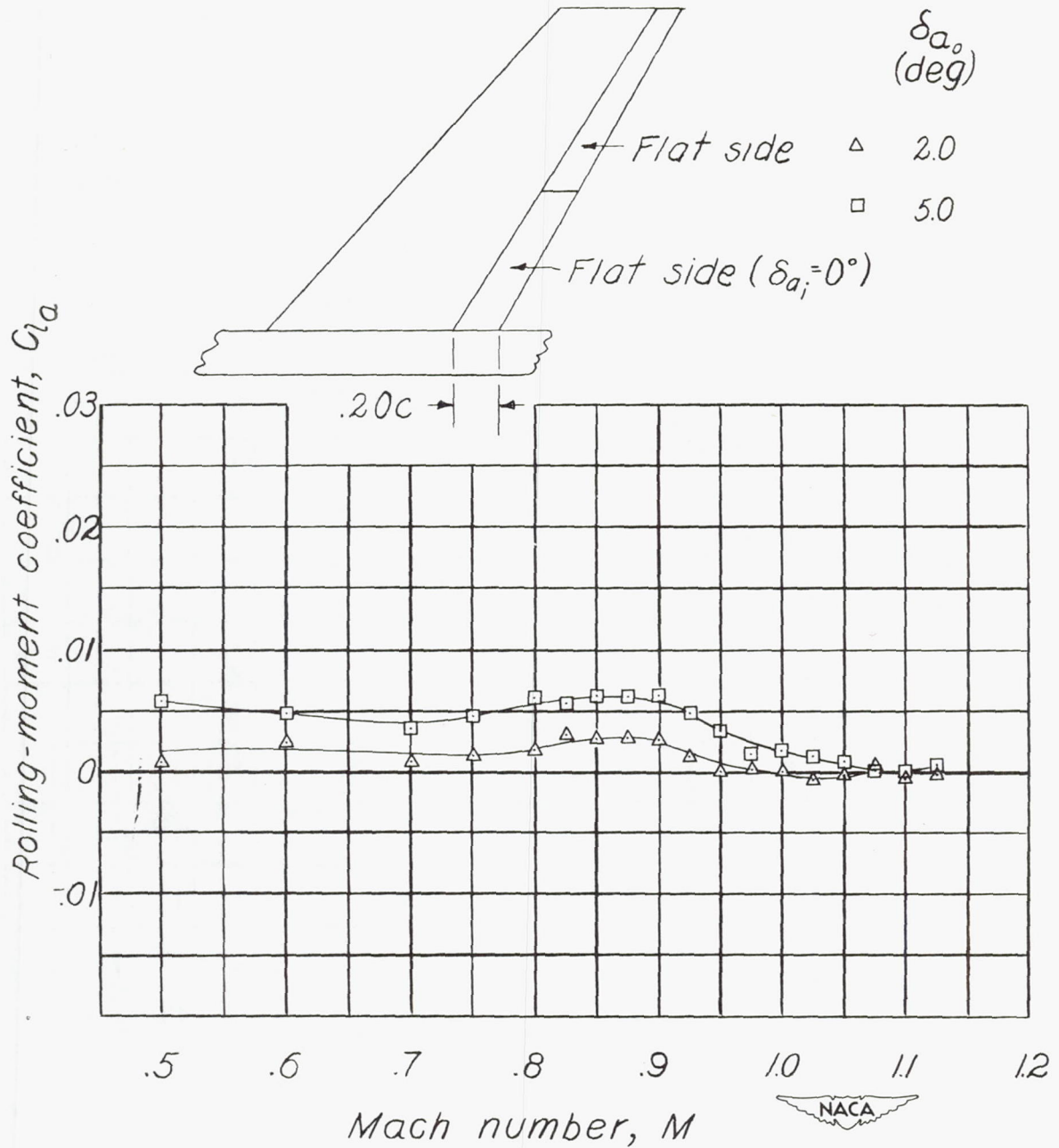


Figure 11.- Variation of rolling-moment coefficient with Mach number for a 0.20-chord flat-sided outboard aileron.

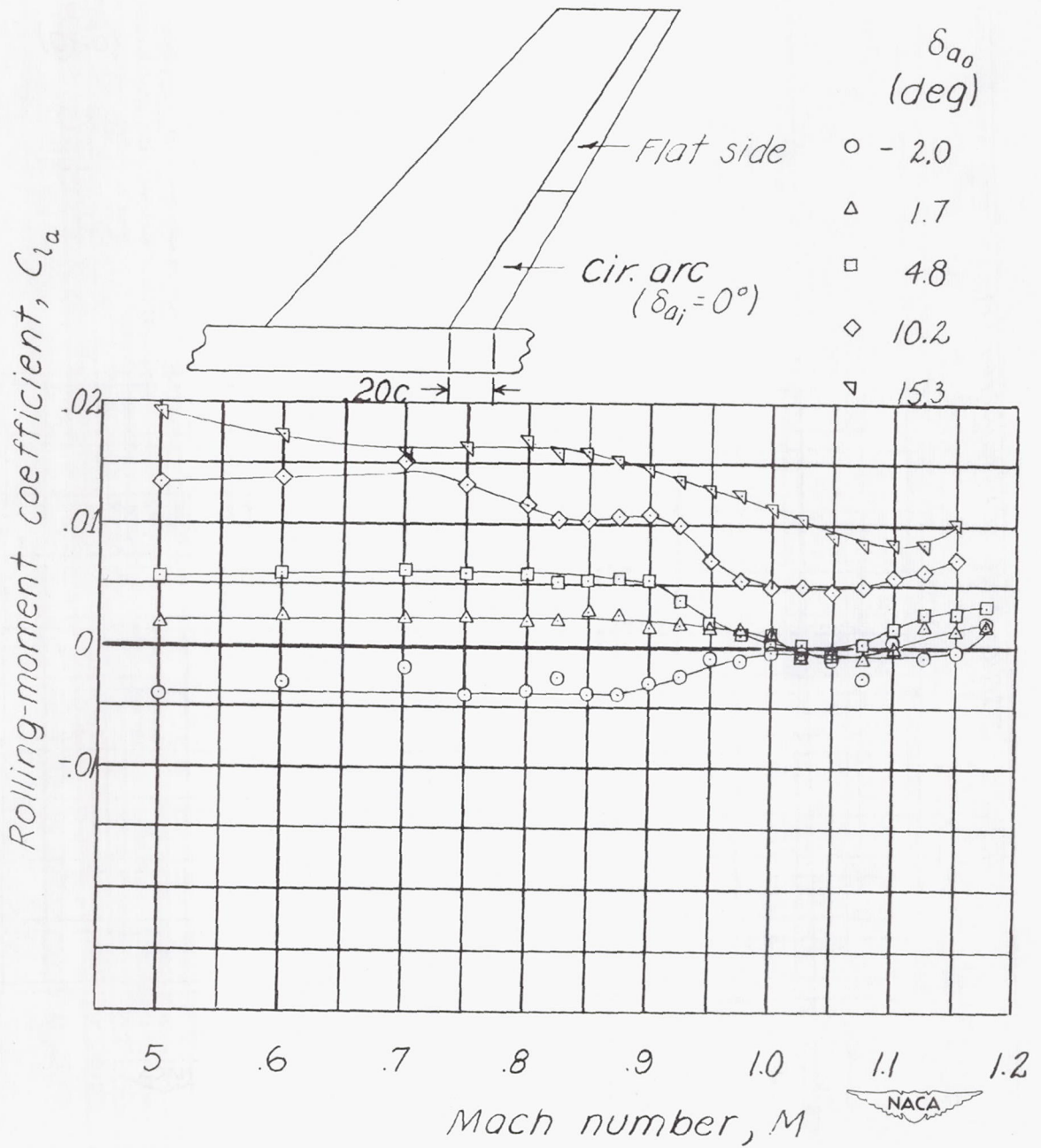


Figure 12.- Variation of rolling-moment coefficient with Mach number for a 0.20-chord flat-sided outboard aileron.

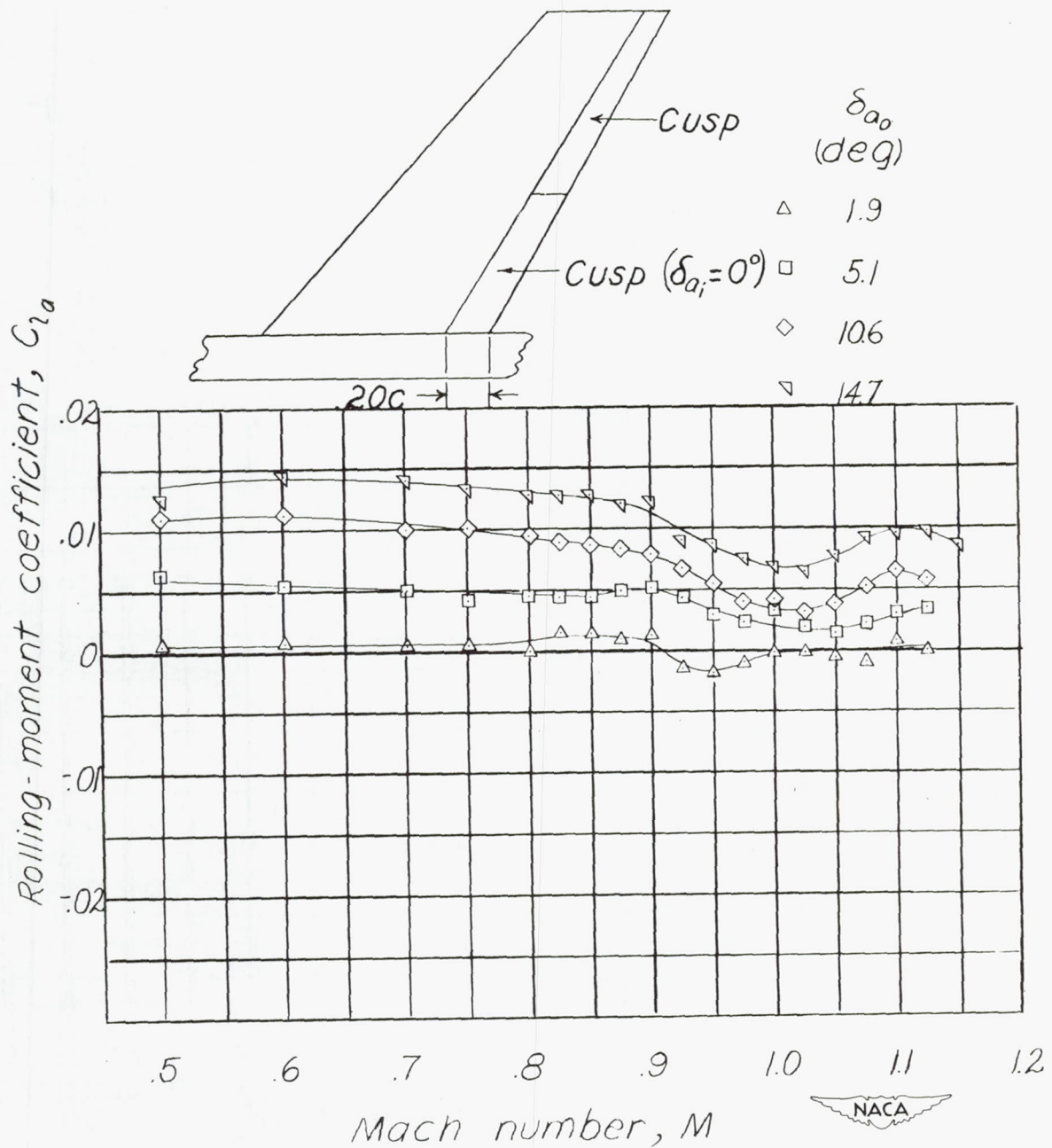


Figure 13.- Variation of rolling-moment coefficient with Mach number for a 0.20-chord cusp outboard aileron.

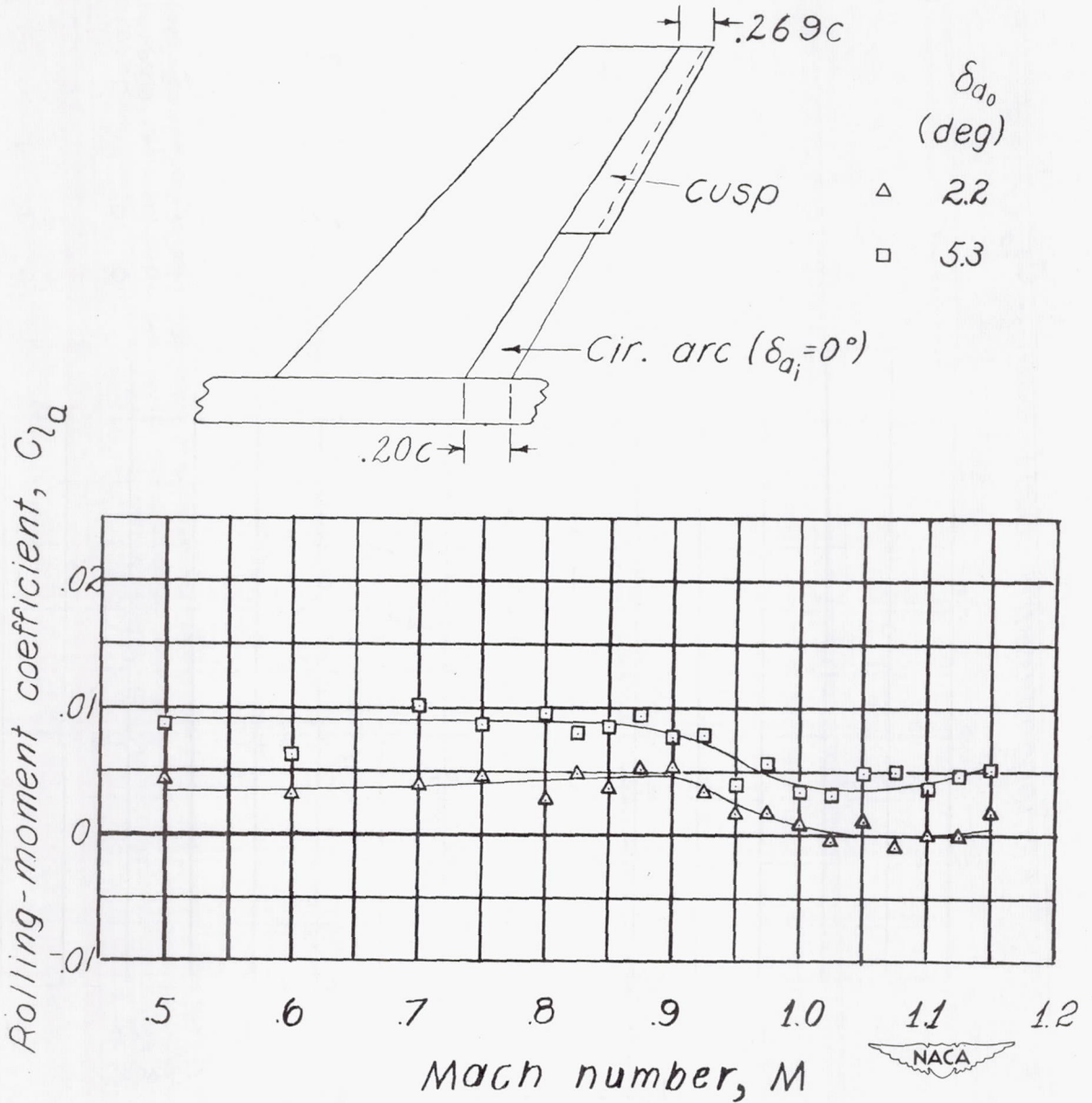


Figure 14.- Variation of rolling-moment coefficient with Mach number for a 0.269-chord cusp outboard aileron.

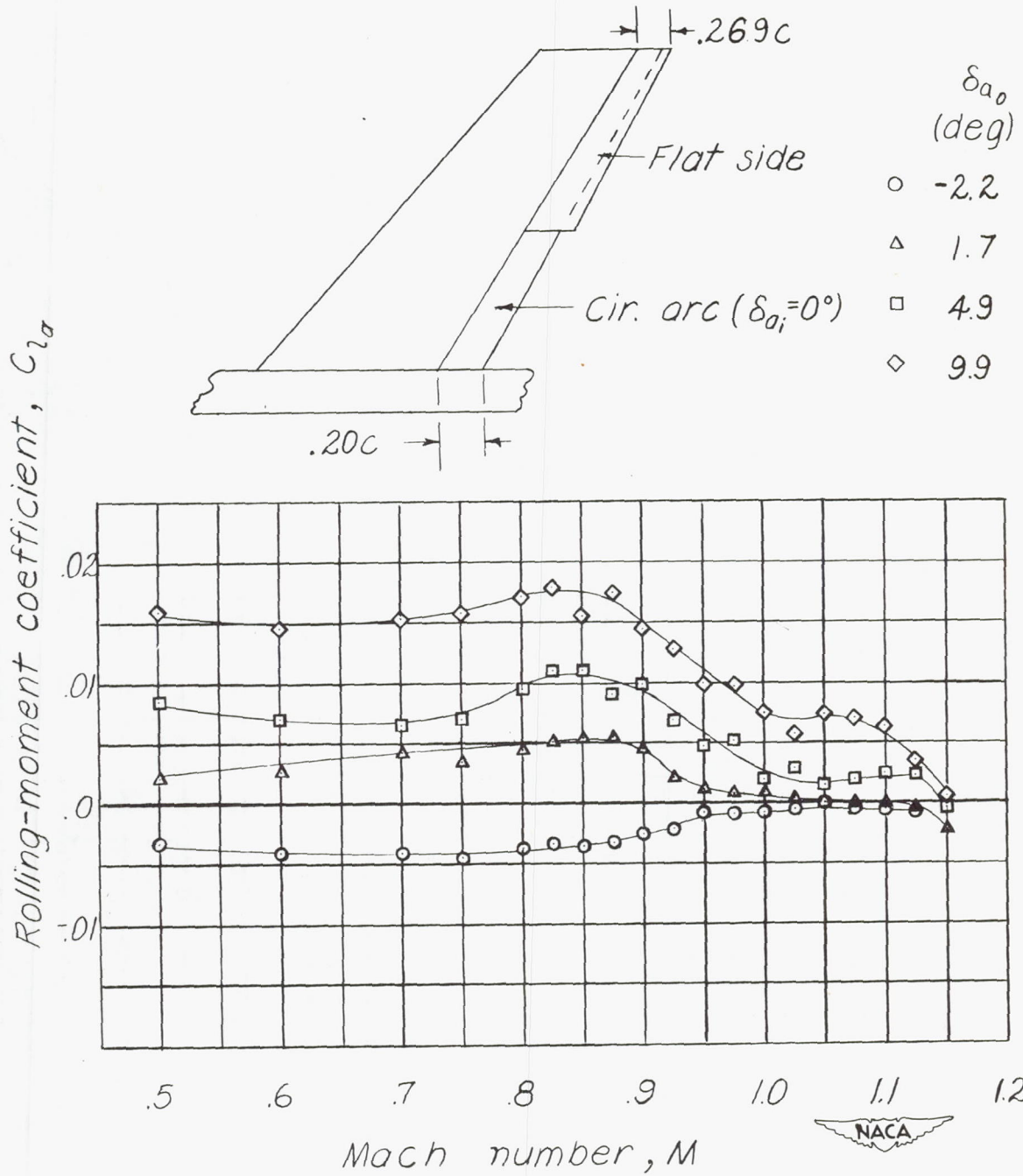


Figure 15.- Variation of rolling-moment coefficient with Mach number for a 0.269-chord flat-sided outboard aileron.

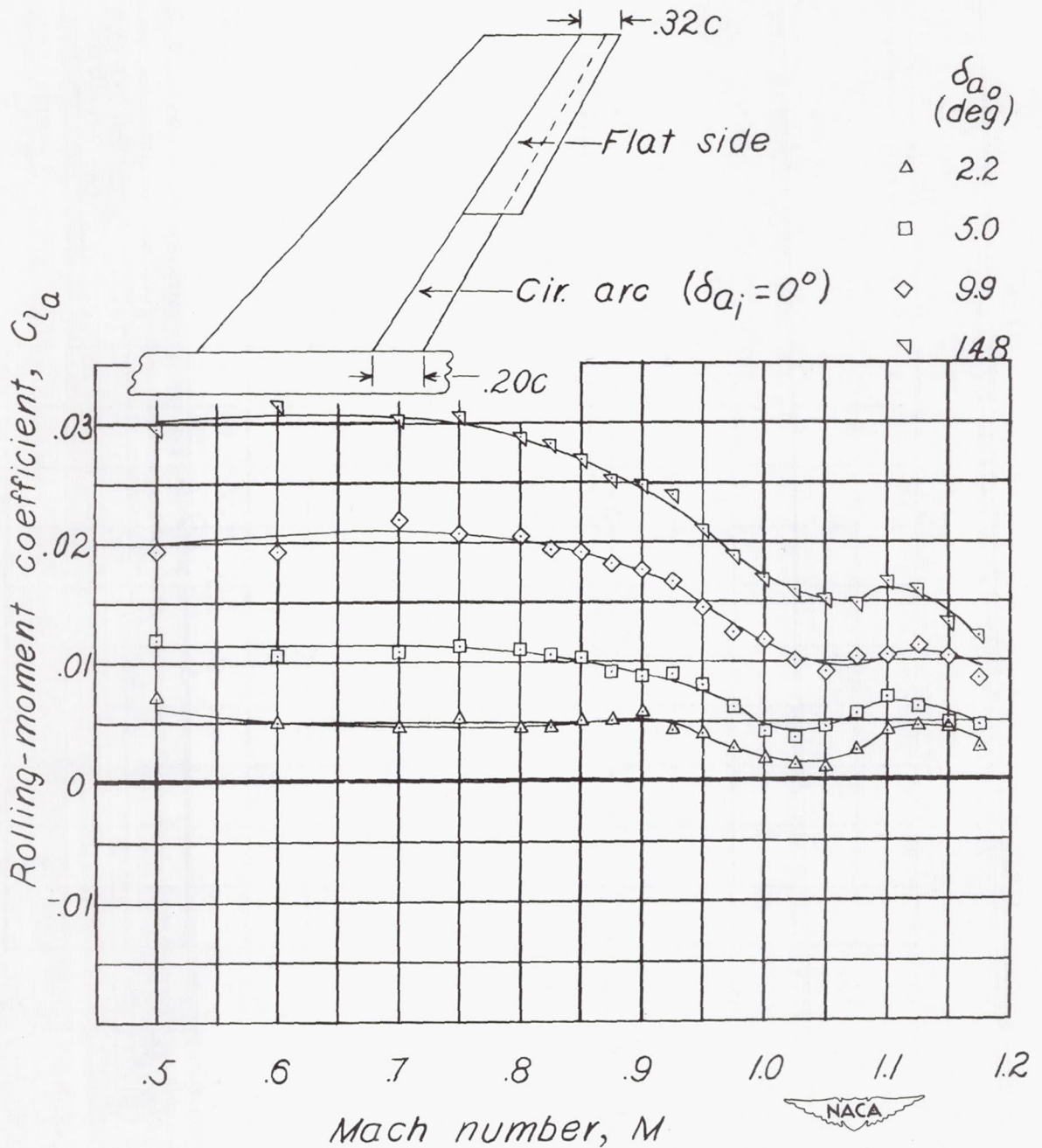


Figure 16.- Variation of rolling-moment coefficient with Mach number for a 0.32-chord flat-sided outboard aileron.

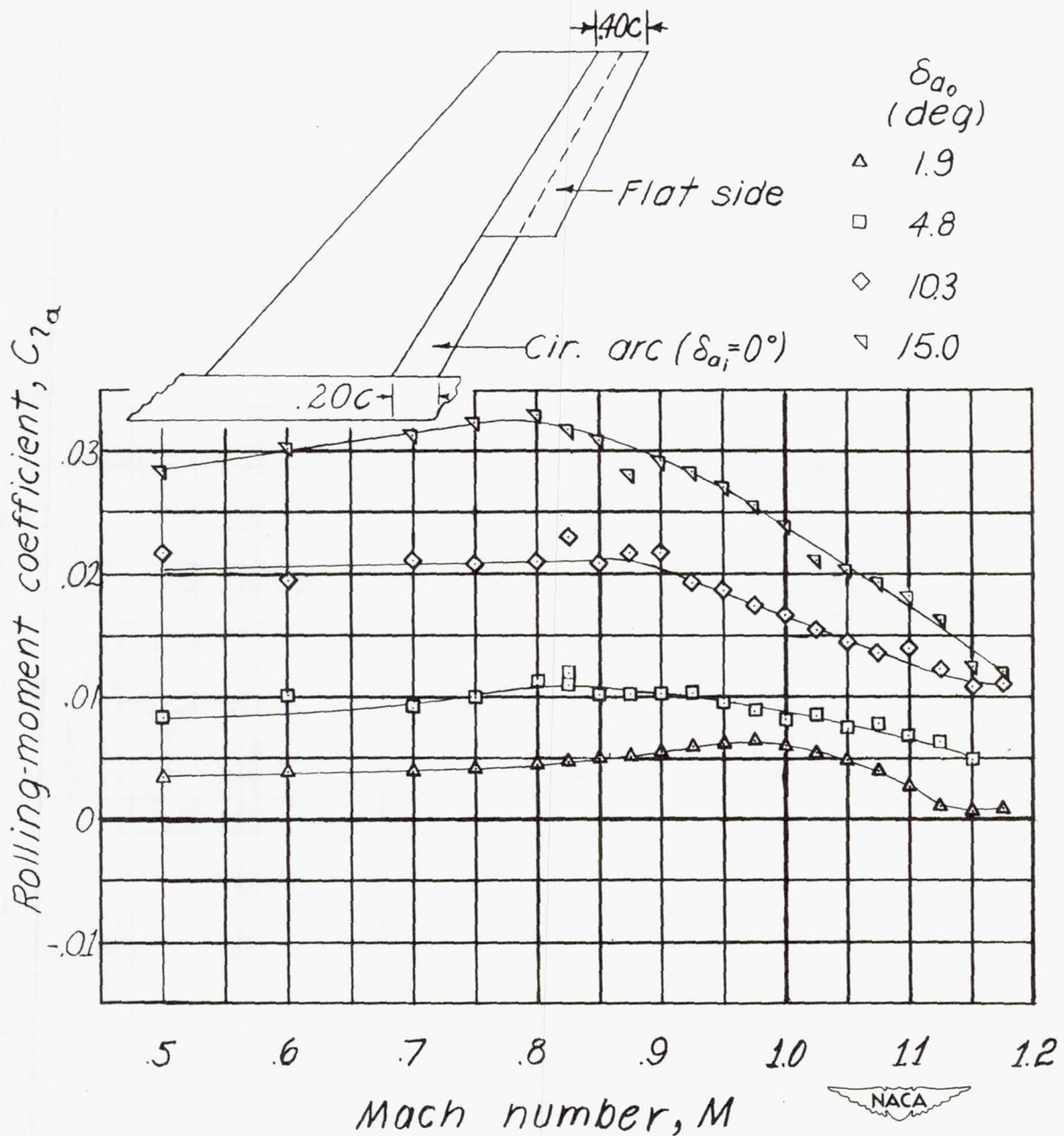


Figure 17.- Variation of rolling-moment coefficient with Mach number for a 0.40-chord flat-sided outboard aileron.

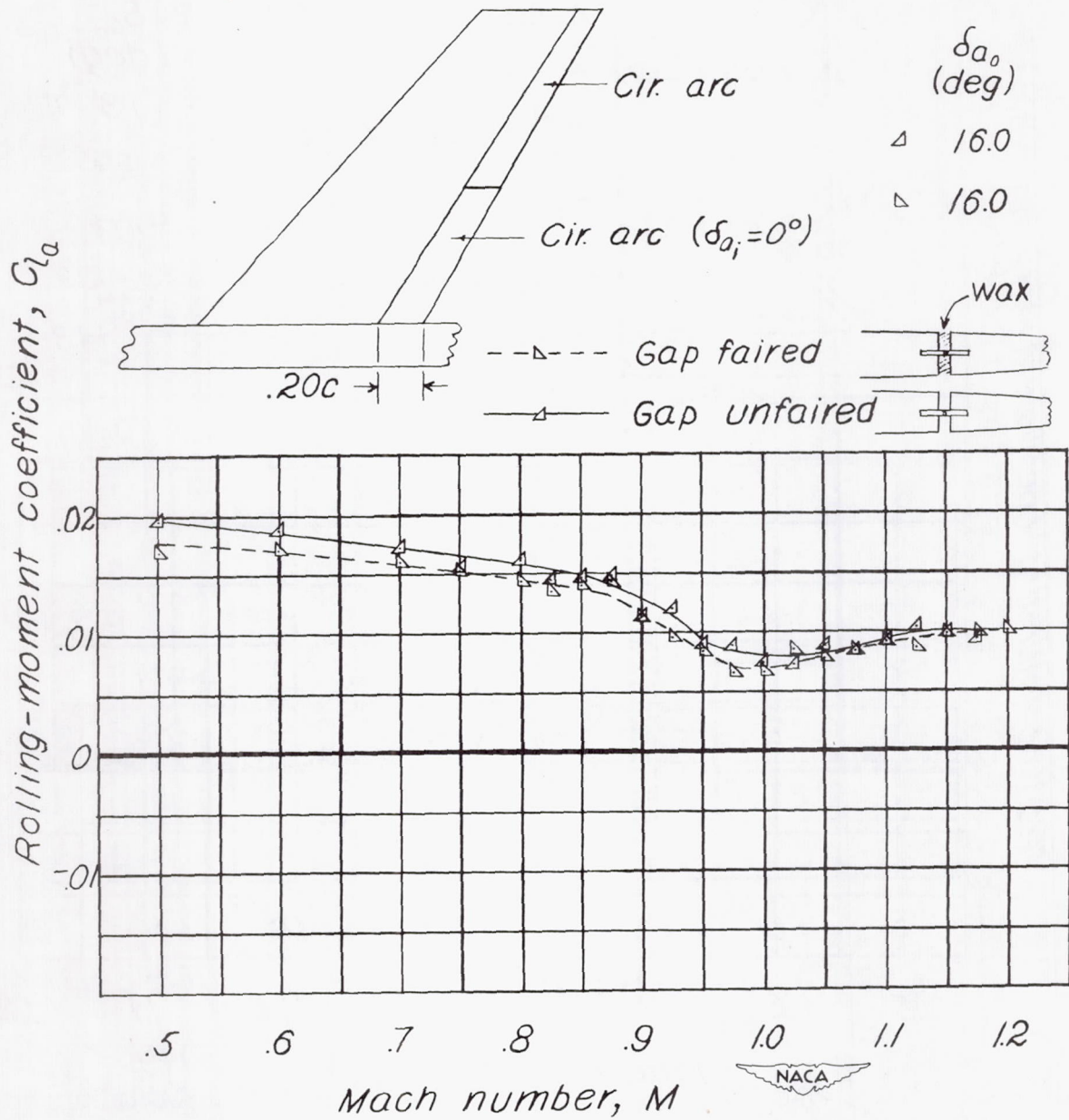


Figure 18.- Variation of rolling-moment coefficient with Mach number for a 0.20-chord circular-arc outboard aileron with and without aileron gap.

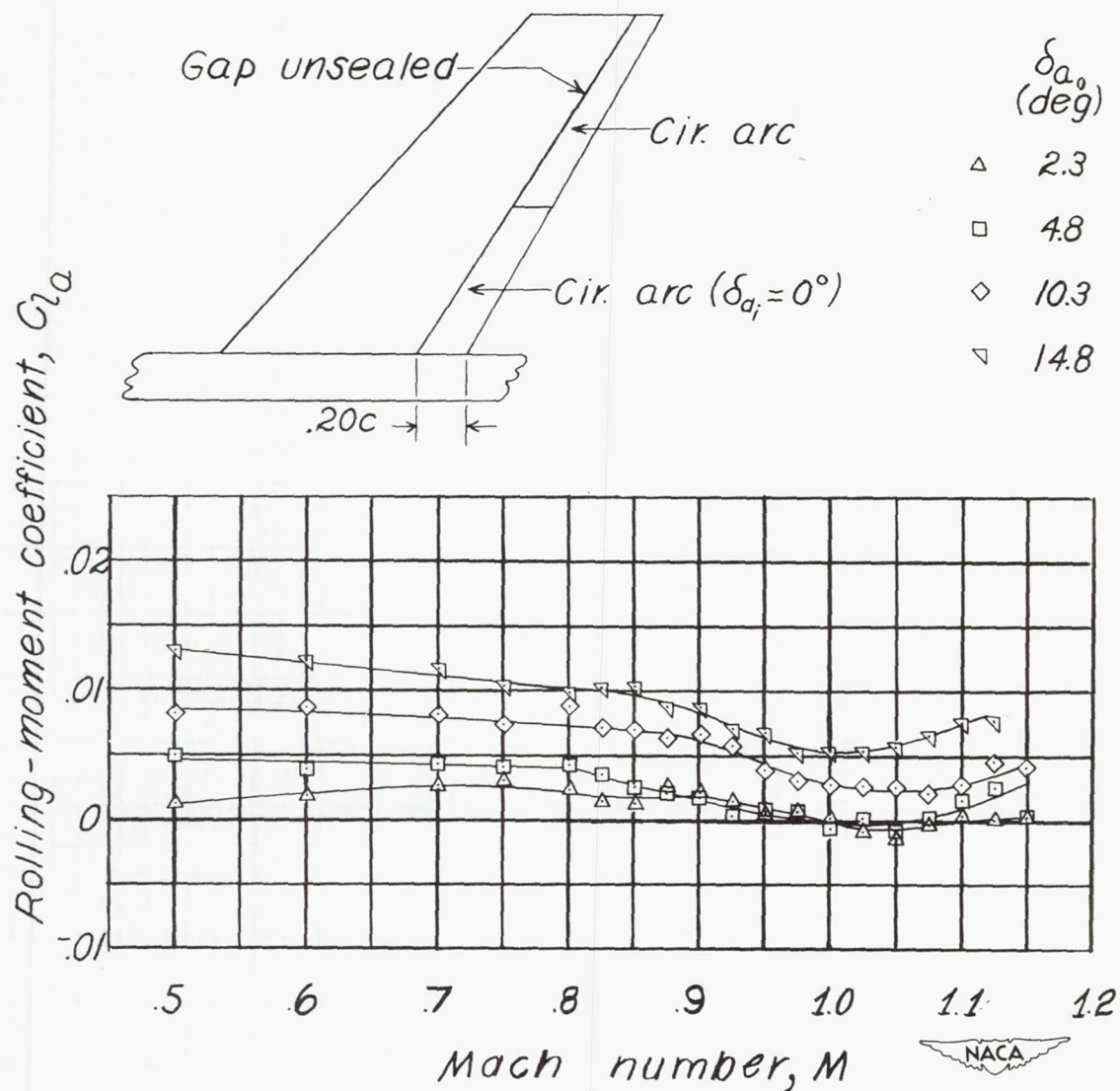


Figure 19.- Variation of rolling-moment coefficient with Mach number for a 0.20-chord circular-arc outboard aileron with unsealed gap.

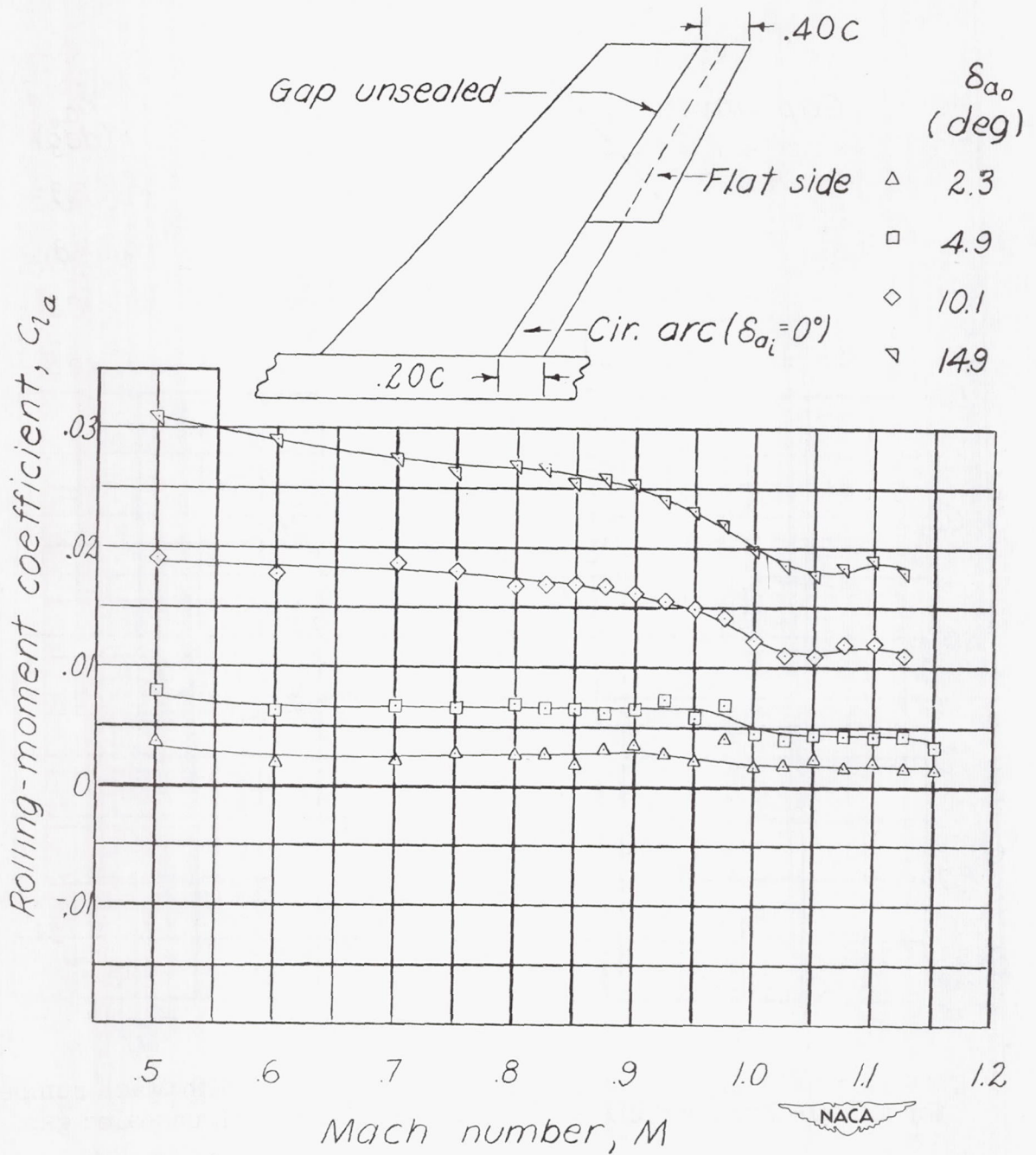


Figure 20.- Variation of rolling-moment coefficient with Mach number for a 0.40-chord flat-sided outboard aileron with unsealed gap.

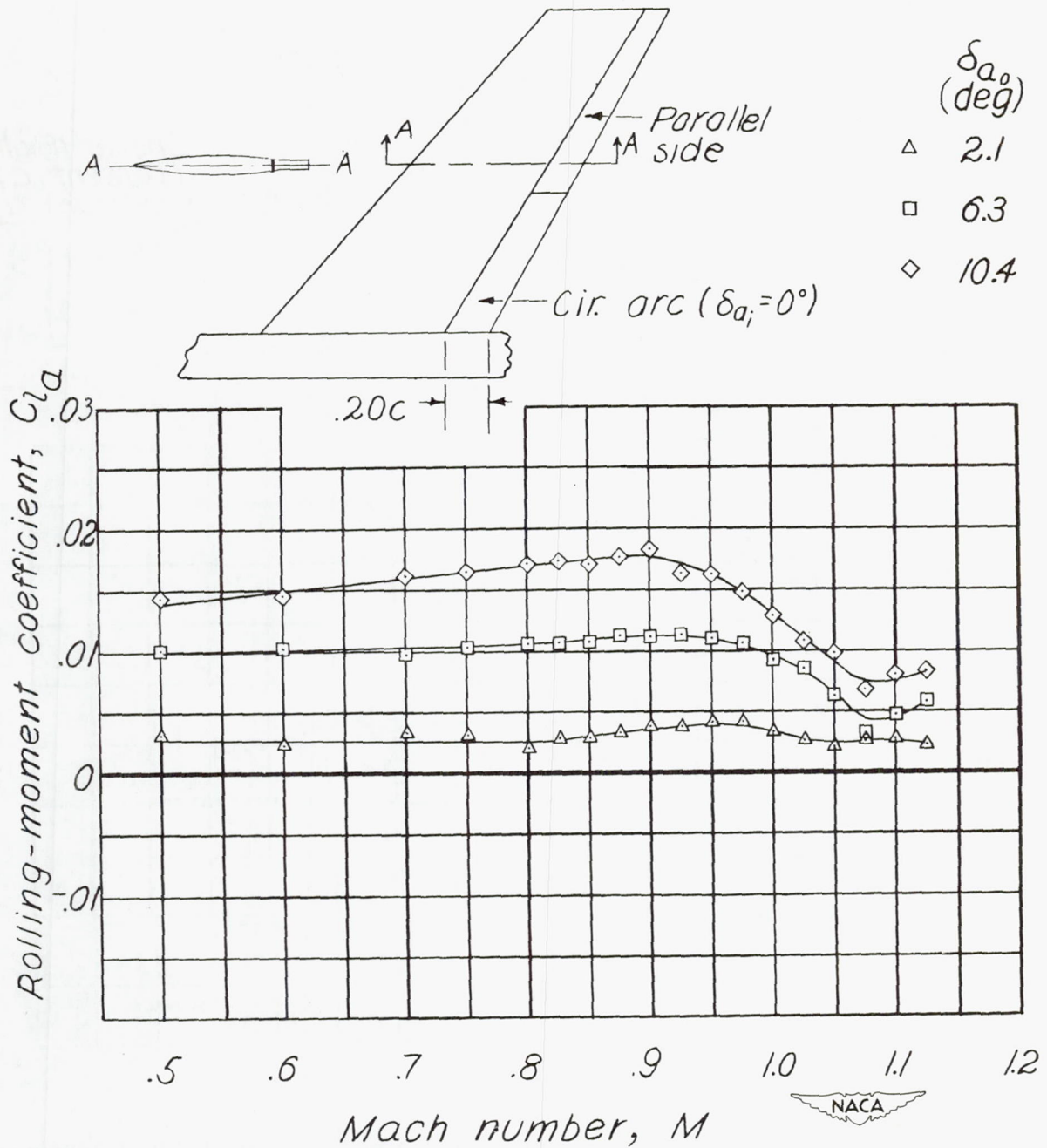


Figure 21.- Variation of rolling-moment coefficient with Mach number for a 0.20-chord parallel-sided outboard aileron.

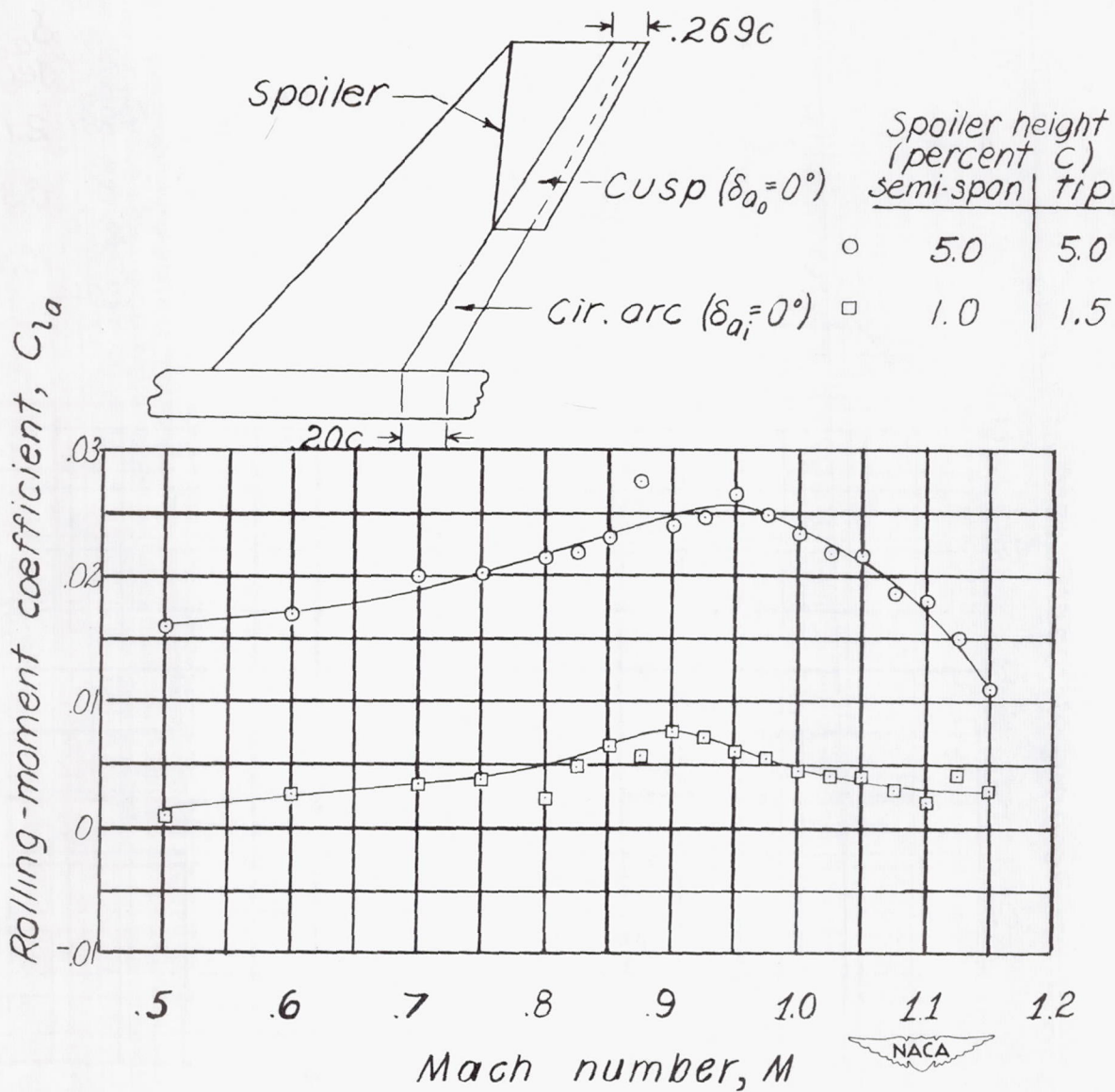


Figure 22.- Variation of rolling-moment coefficient with Mach number for a 0.50-semispan outboard spoiler.

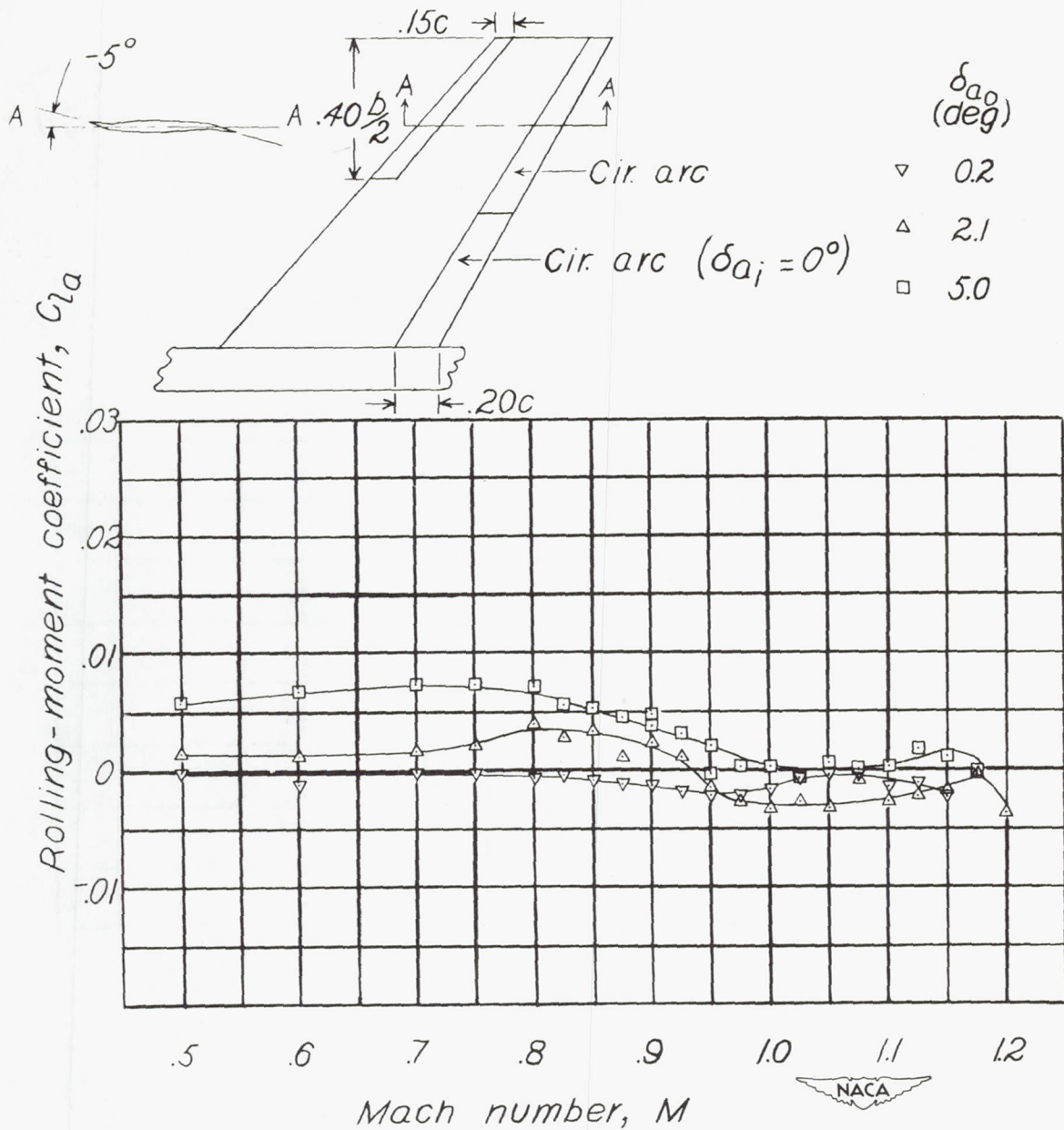


Figure 23.- Variation of rolling-moment coefficient with Mach number for a 0.20-chord circular-arc outboard aileron with leading-edge outboard flap deflected -5° .

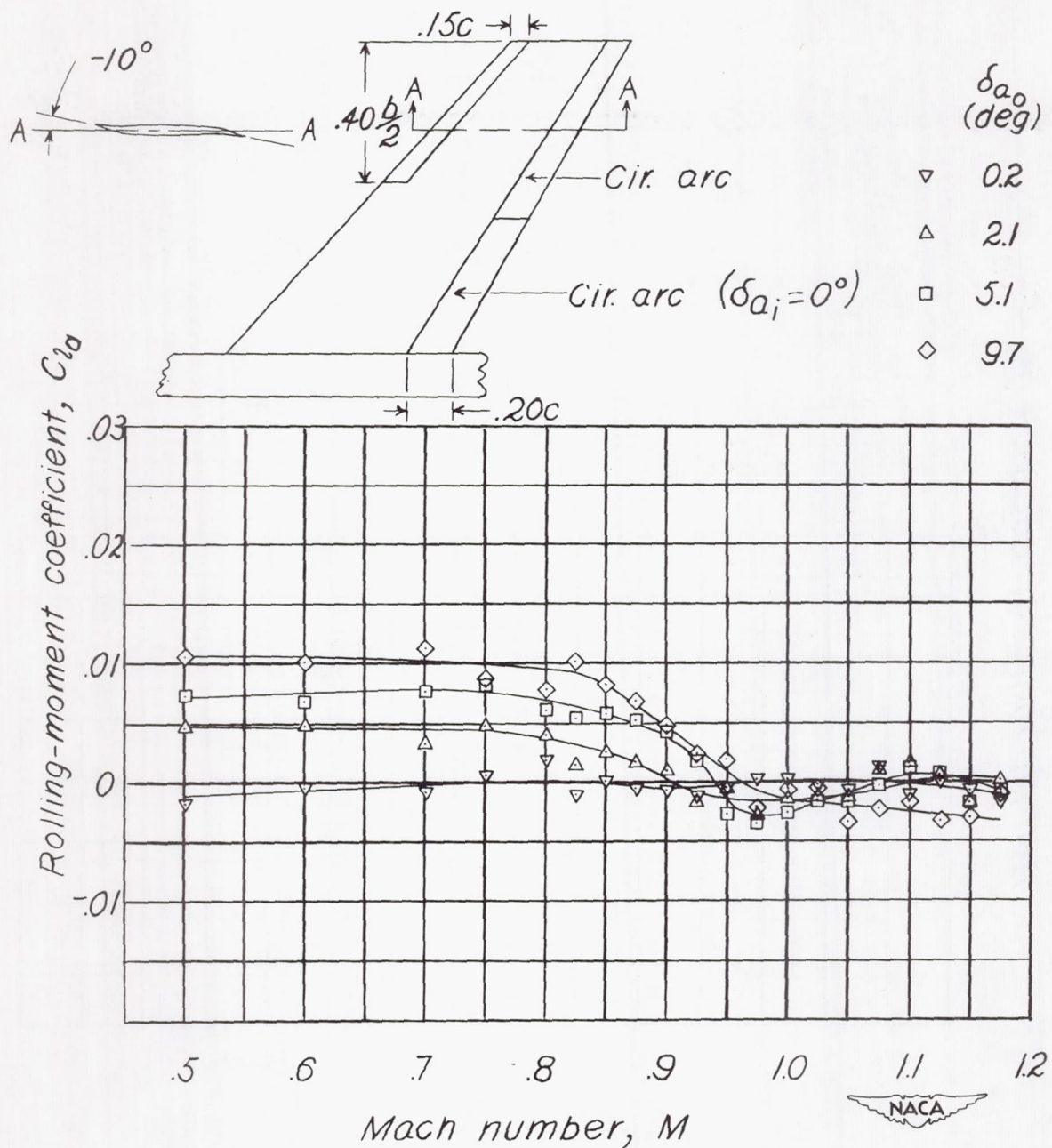


Figure 24.- Variation of rolling-moment coefficient with Mach number for a 0.20-chord circular-arc outboard aileron with leading-edge outboard flap deflected -10° .

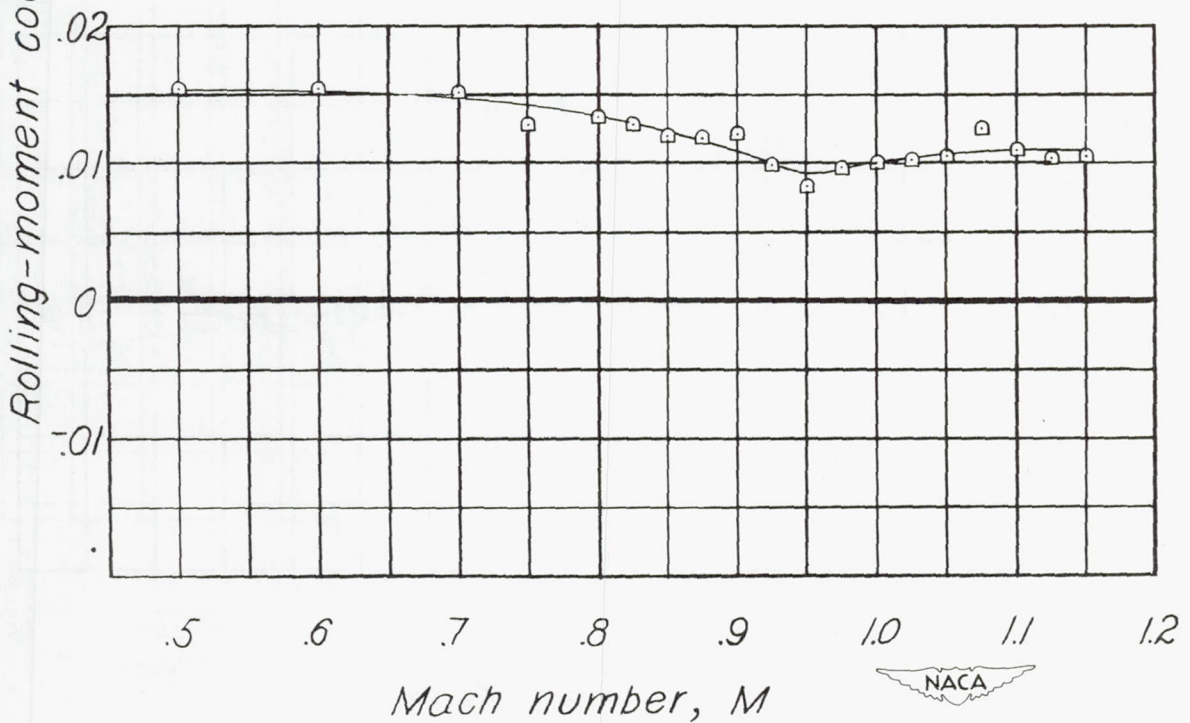
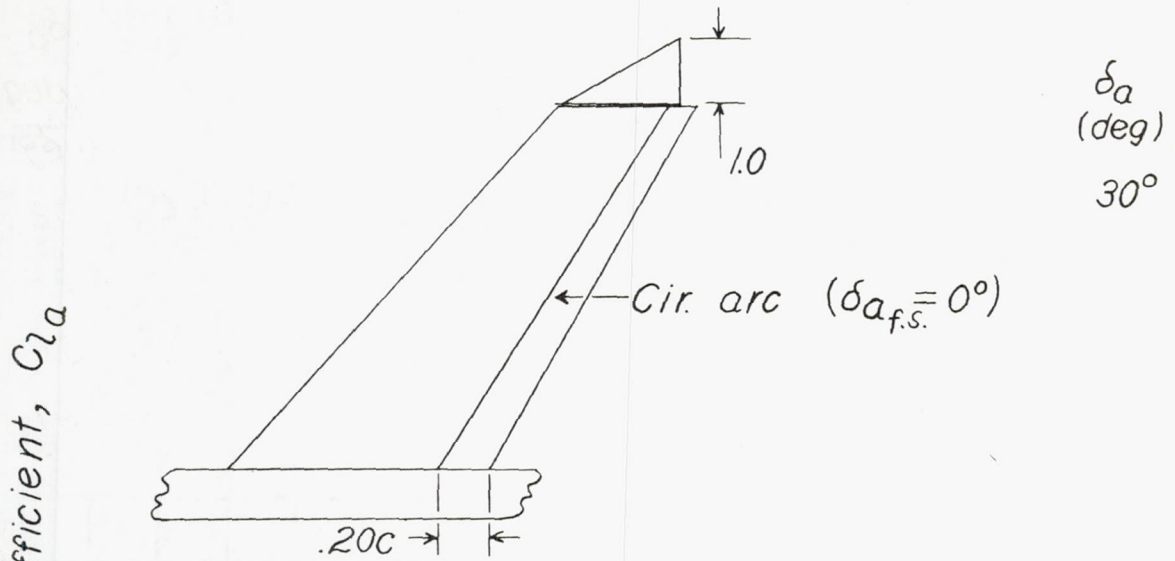


Figure 25.- Variation of rolling-moment coefficient with Mach number for a triangular tip aileron deflected 30° .

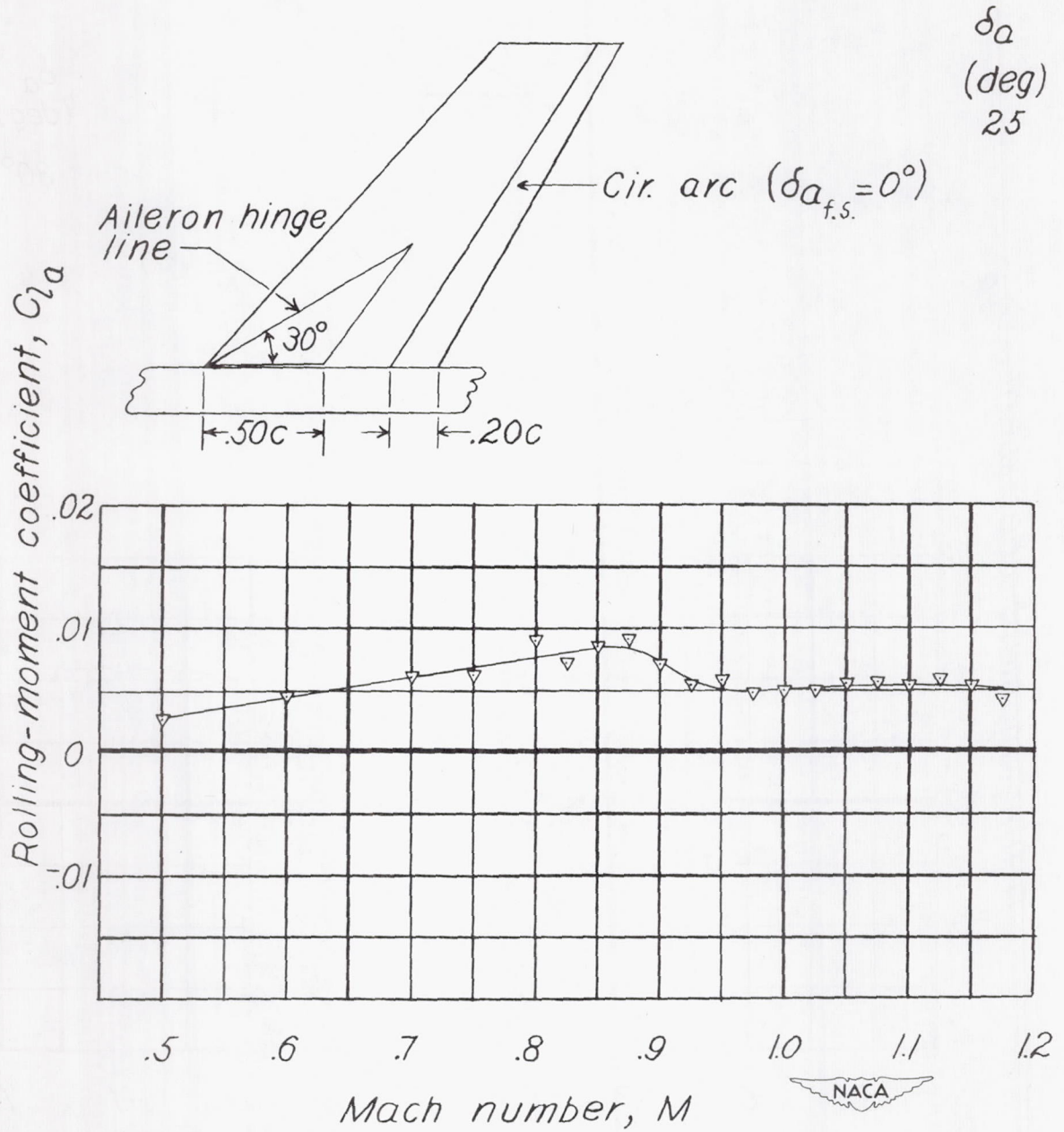


Figure 26.- Variation of rolling-moment coefficient with Mach number for a triangular inboard aileron.

